Resilience Enhancement of Coordinated Transmission and Distribution System via Risk-based Decentralized Planning Against Typhoons

Zijun Yuan, Heng Zhang, Haozhong Cheng, Lu Liu, Jianqin Liu, Ying Wang, and Defu Cai

***Abstract*—The occurrence of high-impact low-probability (HILP) natural disasters such as typhoons poses a significant threat to the secure operation of transmission and distribution (T&D) network system. Simultaneously, the rapid advancement in power distribution grid technologies contributes to the efficient interaction between transmission network and distribution network, thereby providing more possibilities for defending against disasters from a cooperative perspective in T&D network system. To explore the resilience enhancement potential of coordinated transmission and distribution system (CTDS) in defense of probabilistic typhoon impact, a risk-based decentralized planning model for CTDS is proposed aiming at mitigating load reduction at the transmission-distribution level considering random typhoon impact. The planning decision incorporates the investment in transmission line hardening, transmission network expansion at transmission level and distribution line hardening, mobile emergency generator (MEG) deployment as well as automatic switch deployment at distribution level. To address the decentralized model with multiple scenarios, a novel integrated solution procedure is proposed which embeds the alternating direction method of multipliers (ADMM) into a bundle-based progressive hedging algorithm (BPHA), thereby enhancing computation efficiency. The effectiveness and superiority of the proposed resilience enhancement method is demonstrated on a T6D3 system and a T118D7 system.**

***Index Terms*—Coordinated transmission and distribution system, decentralized planning, progressive hedging algorithm, resilience, risk mitigation.**

NOMENCLATURE

Sets and Indices

$s \in \{\mathcal{S}, \bar{\mathcal{S}}, \tilde{\mathcal{S}}\}$	Set of scenarios, normal scenarios and extreme scenarios.
$l \in \{\Gamma^{\mathrm{TNS}}, \Gamma^{\mathrm{TNS*}}\}$	Set of existing and candidate transmission lines.
$g \in \Omega^{\mathrm{TNS}}$	Set of CGUs in TNS.
$w \in \Theta^{\mathrm{TNS}}$	Set of wind farms in TNS.
$b \in \Xi^{\mathrm{TNS}}$	Set of buses in TNS.
$o \in \Xi^{\mathrm{TD}}$	Set of the boundary buses in TNS.
$ij \in \Gamma^{\mathrm{DNS}}$	Set of distribution lines in DNS.
$k \in \Omega^{\mathrm{DNS+}}$	Set of candidate MEGs in DNS.
$i \in \Xi^{\mathrm{DNS}}$	Set of nodes in DNS.
$o \in \Xi_m^{\mathrm{DT}}$	Set of the boundary nodes in DNS.
$d \in \mathcal{B}$	Set of scenario bundles.

Parameters

$C_{\mathrm{inv,ini}}^{\mathrm{TNS}}, C_{\mathrm{inv}}^{\mathrm{TNS}}$	Investment cost and annualized investment cost for TNS.
$C_{\mathrm{inv,ini}}^{\mathrm{DNS}}, C_{\mathrm{inv}}^{\mathrm{DNS}}$	Investment cost and annualized investment cost for DNS.
$C_{\mathrm{ope},s}^{\mathrm{TNS}}, C_{\mathrm{ope},s}^{\mathrm{DNS}}$	Operation cost of TNS and DNS.
$\Psi_s^{\mathrm{TNS}}, \Psi_s^{\mathrm{DNS}}$	Total load shedding of TNS and DNS under typhoon scenarios.
$C_l^{\mathrm{H,TNS}}, C_l^{\mathrm{L,TNS}}$	Unit investment cost for transmission line hardening and construction.
$C_{ij}^{\mathrm{H,DNS}}, C_k^{\mathrm{Ginv}}$	Unit investment cost for distribution line hardening, MEG deployment in DNS.
C_{ij}^{AS}	Investment cost for automatic switch.
$C_g^{\mathrm{su,TNS}}, C_g^{\mathrm{op,TNS}}$	Unit startup cost and operation cost of CGU.
$C^{\mathrm{ls,TNS}}, C^{\mathrm{wc,TNS}}$	Unit load shedding cost and wind curtailment cost in TNS.
$C^{\mathrm{op,DNS}}, C^{\mathrm{om,DNS}}$	Unit operation cost of conventional DG and MEG in DNS.
$C^{\mathrm{buy,DNS}}, C^{\mathrm{ls,DNS}}$	Unit upstream purchase cost and load shedding cost in DNS.
$C^{\mathrm{wc,DNS}}$	Unit wind curtailment cost in DNS.
$\zeta^{\mathrm{H,TNS}}, \zeta^{\mathrm{H,DNS}}$	Budget of hardening cost in TNS and DNS.
$D_b^{\mathrm{TNS}}, D_i^{\mathrm{DNS}}$	Active load demand in TNS and DNS.
$F_l^{\max}, B_l$	Transmission line capacity and susceptance.
$P_g^{\mathrm{G}\max}, P_g^{\mathrm{G}\min}$	Maximum/minimum power output of CGU.
$\kappa_s, \vartheta_s^{\mathrm{TNS}}$	Load growth factor in CTDS and wind farm capacity growth factor in TNS.
$P_w^{\mathrm{W}\max}, c_w^{\mathrm{W,TNS}}$	Capacity and forecast power proportion of wind farm.
$\xi_{l,s}^{\mathrm{TNS}}, \xi_{ij,s}^{\mathrm{DNS}}$	Line failure status in TNS and DNS.
$Q_i^{\mathrm{DNS}}, \vartheta_s^{\mathrm{DNS}}$	Reactive load and wind-based DG capacity growth in DNS.

This work was sponsored by National Natural Science Foundation of China (No. U23B6006, 52307120). (*Corresponding author: Heng Zhang*).

Zijun Yuan, Heng Zhang, Haozhong Cheng, Lu Liu are with Key Laboratory of Control of Power Transmission and Conversion, Ministry of Education, Shanghai Jiao Tong University, Shanghai 200240, China (e-mail: yuanzijun_306@sjtu.edu.cn; zhangheng_sjtu@sjtu.edu.cn; hzcheng@sjtu.edu.cn; liulu52@sjtu.edu.cn).

Jianqin Liu and Ying Wang are with State Grid Economic and Technological Research Institute., Ltd, Beijing 102209, China.

Defu Cai is with Electric Power Research Institute of Hubei Power Grid Corporation, Wuhan 430048, China.

R_{ij}, X_{ij}	Distribution line resistance and reactance.
$I_{ij}^{\max}, I_{ij}^{\min}$	Maximum/minimum current amplitude.
$V_i^{\max}, V_i^{\min}$	Maximum and minimum voltage magnitude.
$P_i^{\mathrm{CD}\max}, P_i^{\mathrm{CD}\min}$	Maximum/minimum active power output of conventional DG in DNS.
$Q_i^{\mathrm{CD}\max}, Q_i^{\mathrm{CD}\min}$	Maximum/minimum reactive power output of conventional DG in DNS.
$P_k^{\mathrm{MG}\max}, P_k^{\mathrm{MG}\min}$	Maximum/minimum active power output of MEG in DNS.
$Q_k^{\mathrm{MG}\max}, Q_k^{\mathrm{MG}\min}$	Maximum/minimum reactive power output of MEG in DNS.
$P_i^{\mathrm{WD}\max}, c^{\mathrm{WD,DNS}}$	Capacity and forecast power proportion of wind-based DG.
$\phi_o, \phi_i^{\mathrm{WD}}$	Power factors in DNS.
τ_{ij}	Binary parameter indicating whether distribution line is tie-line (1) or not (0).
π_s, π_d	Probability of scenario and scenario bundle.
Δ^{du}	Duration in a planning year.
Variables	
$x_l^{\mathrm{H,TNS}}, x_l^{\mathrm{L,TNS}}$	Binary variable indicating whether transmission line is hardened/built (1) or not (0).
$SU_{g,s}$	Binary variable indicating whether CGU is started up (1) or not (0).
$P_{g,s}^{\mathrm{G}}, P_{w,s}^{\mathrm{W}}$	Power output of CGU and wind farm.
$r_{w,s}^{\mathrm{W,TNS}}, r_{i,s}^{\mathrm{WD,DNS}}$	Power curtailed of wind farm and wind-based DG.
$P_{o,s,m}^{\mathrm{TD}}, P_{o,s,m}^{\mathrm{DT}}$	Transmitted power in TNS and DNS.
$f_{l,s}$	Power flow of transmission line *l* in TNS.
$\theta_{se(l),s}, \theta_{re(l),s}$	Voltage angle at the sending bus and receiving bus in TNS.
$r_{b,s}^{\mathrm{U,TNS}}, r_{i,s}^{\mathrm{U,DNS}}$	Unserved load in TNS and DNS.
$x_{ij}^{\mathrm{H,TNS}}, x_k^{\mathrm{MG}}, x_{ij}^{\mathrm{AS}}$	Binary variables indicating whether distribution line is hardened (1) or not (0), MEG is deployed (1) or not (0), and automatic switch is deployed (1) or not (0).
$P_{i,s}^{\mathrm{CD}}, Q_{i,s}^{\mathrm{CD}}$	Active/reactive power output of conventional DG in DNS.
$P_{i,s}^{\mathrm{WD}}, Q_{i,s}^{\mathrm{WD}}$	Active/reactive power output of wind-based DG in DNS.
$p_{ij,s}, q_{ij,s}$	Active/reactive power flow in DNS.
$P_{i,k,s}^{\mathrm{MG}}, Q_{i,k,s}^{\mathrm{MG}}$	Active and reactive power output of MEG.
$\varphi_{i,k,s}$	Binary variable indicating whether MEG *k* is accessed to node *i* (1) or not (0).
$L_{ij,s}, U_{i,s}$	Square of current and voltage magnitude.
$\alpha_{ij,s}$	Binary variable indicating whether the distribution line is operating (1) or not (0).
$\beta_{ji,s}$	Binary variable indicating whether the node *i* is the parent node (1) of node *j* or not (0).

I. Introduction

With the degradation of the ecological environment, natural disasters such as typhoons, floods and ice storms are causing more significant disruptions to power transmission and distribution which play pivotal roles in the power system. For example, the strike of Super Typhoon Lekima in 2019 caused a total of 72 substations above 35 kV in China to lose power and 535,500 customers to suffer power outages. Simultaneously, as the smart grid technology advances rapidly, distribution network is gradually transitioning to the active distribution network with distributed resources, thereby enhancing the benefits of interconnection between transmission network system (TNS) and distribution network system (DNS) [1]. This contributes to improving the power system defense capability against natural disasters from the level of transmission and distribution cooperation [2], [3].

System resilience can be enhanced at both transmission and distribution levels from the perspective of planning [4]. In general, conducting preventive resilient planning such as hardening planning [5], expansion planning [6] or procuring emergent equipment [7] and smart grid technologies [8] plays an important role in defense of natural disasters. In terms of transmission network resilience enhancement, a two-stage stochastic formulation [9] and a data-driven robust optimization approach [10] are proposed to obtain the optimal defense hardening plan for transmission lines. Investment options include the hardening of transmission lines, generators and substations. Transmission expansion planning is also regarded as a measure to boost resilience along with hardening planning, generation expansion planning [12] or distributed energy resources planning [13], and both the operation cost under normal condition and outage cost under emergency condition are minimized. Distribution network resilience can be enhanced via multiple resources including distribution line hardening [14], distributed generation (DG) allocation [15], sectionalizing switch planning [16] and mobile energy resources planning such as mobile emergency generator (MEG) deployment [17], etc. In [18], a robust distribution line hardening planning model is presented with DG allocation and energy storage deployment respectively to reduce load loss under disasters. The above distribution network resources can also be taken into account comprehensively to increase resiliency while saving costs [19], [20], [21]. However, the aforementioned literature is unable to consider the integration of resilience assets across the entire transmission and distribution (T&D) network systems for planning, as it solely focuses on optimizing investment portfolios at the individual level of TNS or DNS.

In actual power systems, the efficient and more frequent interaction between TNS and DNS has provided significant benefits for addressing issues of the overall system [22], [23]. And the coordinated planning of T&D network systems is also conducive to enhancing the overall system performance, such as economic [24], reliability [25] and voltage stability [26]. A distributed second-order cone programming-based model for the integrated planning of TNS and DNS is formulated in [27] to allow only the exchange of power output information at the boundary buses, which safeguards the data privacy. By using an analytical target cascading method, a decentralized stochastic optimization model is proposed in [28] for the expansion planning of integrated transmission and distribution network considering DG penetration. In light of the potential benefits brought by the coordination between TNS and DNS,

TABLE I
COMPARISON OF REPRESENTATIVE RESILIENT PLANNING STUDIES IN T&D NETWORK SYSTEMS

Ref.	TNS resilience measures		DNS resilience measures			Extreme and normal scenarios	Risk management	TNS&DNS coordination
	Hardening	Expansion	Hardening	MEG/DG	Automatic switch			
[6]	×	√	×	×	×	×	×	×
[9], [10]	√	×	×	×	×	×	×	×
[11]	√	√	×	×	×	√	×	×
[12]	×	√	×	×	×	√	×	×
[14]	×	×	√	×	×	×	×	×
[15],[17]	×	×	×	√	×	√	×	×
[18]	×	×	√	√	×	×	×	×
[21]	×	×	√	√	√	√	×	×
[34],[35]	×	×	√	√	×	×	√	×
[29]	√	×	√	×	√	×	×	√
[30]	√	×	√	×	×	×	×	√
This paper	√	√	√	√	√	√	√	√

the capability of cooperative planning of coordinated transmission and distribution system (CTDS) in withstanding typhoon disasters is worth excavating to enhance the resilience of the overall system. Substation proactive protections with installing Tiger Dams within transmission and distribution system are coordinated in [29] to defend the impact of floods. And a distributionally robust collaborative planning model of TNS and DNS is proposed in [30] to improve restoration during earthquakes. Since only one measure such as hardening is considered in these preventive planning studies, the cost-effective plan for the overall system cannot be achieved.

When considering the economic aspects of investing in bolstering resilience, many of the above-mentioned studies primarily conduct planning for natural disaster scenarios while disregarding the electricity growth under normal conditions (e.g., [9], [10], [13], [14], [18], [19], [30]). This may lead to conservative planning schemes which can precipitate a decline in economic performance. In addition, typhoons and other natural disasters are classified as high-impact and low-probability (HILP) events with uncertain nature, it is imperative to estimate their baneful influence on the power system with frequency and severity both considered. In terms of the uncertainties in such events, modeling and addressing natural disaster scenarios without characterizing their tail risks could not provide a risk trade-off perspective. Therefore, the tolerance towards such resulting risk should be considered in resilient planning [31]. For risk analysis, conditional value-at-risk (CVaR) metric has been widely used to describe the risk related to the tail scenarios within a probability distribution [32], [33]. To quantify and manage the risks brought by HILP disasters, resilient distribution network planning models are developed in [34], [35], [36] to obtain the risk-driven plan. And the trade-off between planning decision and resilience performance can be analyzed via the risk measure [37]. But the works in such research address the issues in DNS, neglecting the integration of the assets in CTDS to develop a comprehensive risk-averse strategy for efficiently mitigating the typhoons impact on the entire system.

In general, these researches provide valuable insights on the planning-based resilience enhancement approach of TNS and DNS. However, most of the researches implement the resilience improvement planning at the individual level of TNS or DNS, ignoring the available mutual support between TNS and DNS and the comprehensive utilization of resilience resources. This leads to an imbalanced allocation of resilience resources in CTDS and a limitation in the resilience/economic enhancement planning for TNS and DNS. Besides, overlook of the tail risks associated with HILP disasters as well as normal scenarios in resilience enhancement planning may render an inadequate and inappropriate planning strategy, which is incompatible with the aim of boosting resilience and remaining cost-effective. Given the existing research gap, this paper addresses the issue of mitigating typhoon disasters impact and proposes a risk-based decentralized resilient planning model of CTDS against stochastic typhoons by integrating the assets of T&D network systems. The tail risks of the HILP typhoons are quantified through the CVaR method. The summarization and distinction of the previous representative researches are listed in Table I, emphasizing the spotlight and notable advancements of this paper.

The main contributions of this paper are summarized as:

1) In order to exploit the cooperative potential of resilience resources in T&D network system, a decentralized coordinated planning framework for optimizing CTDS investment is proposed. The framework co-optimizes investment decisions on transmission hardening, expansion in TNS and distribution line hardening, MEG deployment, automatic switch deployment in DNSs, with the power interaction between TNS and DNSs while preserving the data privacy.

2) To mitigate the tail risk in CTDS brought by uncertain typhoon impact, CVaR metric is employed in the resilience enhancement planning model. And planner can draw up investment schemes based on the preferred risk-hedging level. Besides, the uncertainties of system load growth and renewable-based generation capacity (RGC) under normal condition are also modeled via multiple scenarios.

3) To handle the solution efficiency dilemma brought by multiple scenarios in decentralized planning, an integrated iterative solution procedure is developed which embeds the alternating direction method of multipliers (ADMM) into a bundle-based progressive hedging algorithm (BPHA). In this way, the collaboration of TNS and DNSs can be facilitated by limited information exchange within each decomposed scenario bundle, while reducing the computation difficulty.

The remainder of this paper is organized as follows. Section II provides the preliminary requirements for modeling. The model architecture and detailed model formulation are described in Section III. Section IV provides the principle of the solution algorithm and the specific iterative solution procedure. Section V presents the numerical case studies. In

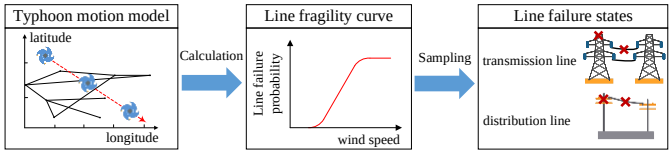

Fig. 1. Line failure states generation under typhoon scenarios.

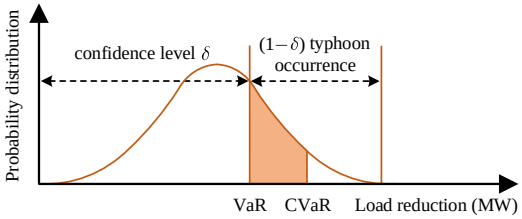

Fig. 2. CVaR representation for typhoon-induced risk.

final, the whole work is concluded in section VI.

II. Preliminary Requirements for Modeling

A. Typhoon-induced impact on transmission/distribution line

Typhoon's spatial-temporal motion can cause a significant impact on the operation status of components in TNS and DNS. In these components, the majority of transmission and distribution lines, which consist of numerous towers and line segments, are highly susceptible to typhoon impacts due to their exposed positions [38]. Hence, in this paper, transmission and distribution lines are considered as the main components affected by typhoons and the typhoon's wind field moving in CTDS is simulated using Batts model [39]. Then, each line fragility curve corresponding to its locational wind speed can be constructed. Then, the maximum line failure probability during typhoon is selected for sampling, which generates the post-typhoon scenarios representing the failure states of transmission lines and distribution lines. The process of scenario generation for typhoon impact is shown in Fig. 1.

B. Risk management by CVaR

The characteristics of typhoon such as moving track and intensity can present variations after its landing due to the inaccuracy prediction. When modeling the uncertainty of typhoon characteristics through a set of scenarios in a probability distribution, the tail probability should also be taken into account which could result in worse load loss. To mitigate such excessive and unexpected losses, a CVaR-based metric is applied for the tail risk measurement under typhoons with stochastic characteristics, and it should be reduced to the minimal. The representation for such typhoon-induced risk is shown in Fig. 2 with CVaR. For typhoons with the HILP nature, VaR represents the expected load reduction value under confidence level δ. On this basis, CVaR represents the expected risk value pertaining to the remaining $1-\delta$ typhoon occurrence region, which denotes the coherent tail risk of load reduction under this typhoon impact and owns a greater value than VaR. Hence, the calculation of CVaR brought by such typhoons can be formulated after the discretization of probability density function, as shown in (1). Wherein, Ψ indicates the system-level total load reduction. π_s^{ty} represents the discretized typhoon scenario probability.

$$\text{CVaR}(\Psi,\delta)=\text{VaR}+\frac{1}{1-\delta}\times\sum_s \pi_s^{\text{ty}}(\Psi-\text{VaR})\big|\Psi\geq\text{VaR} \tag{1}$$

C. Pre-event resilience enhancement measures in CTDS

There are many significative measures for CTDS resilience enhancement, including diverse and comprehensive efforts through the whole pre-event, in-event and post-event stages [4]. In this paper, the work is concentrated on the preparedness before the typhoon disasters occurrence where more efforts should be put into the preventive arrangement and planning to mitigate their adverse impacts. For the purpose of system wide infrastructure pre-protection, the lines spanning the entire CTDS are often inclined to be damaged under typhoons due to many vulnerabilities, including the aforementioned towers being prone to collapse and line segments being susceptible to breakage [39]. This makes hardening of the transmission and distribution lines become a primary response strategy for safeguarding the CTDS [40], thus warranting consideration of line hardening in both the TNS and DNSs. The implementation of physical hardening measures, including vegetation management, undergrounding lines, upgrading poles with more sturdy materials and so forth, can be employed to elevate the ability of equipment to withstand strong winds [41]. For example, 1096 transmission poles and 18000 distribution poles had been replaced with steel or concrete poles in the U.S. to meet the wind loading criteria defined by IEEE's National Electricity Safety Code [42]. In addition to line hardening, transmission expansion can be used to enhance the bulk power grid redundancy under typhoons while guaranteeing the electricity growth demand at the same time. Therefore, hardening and expansion measures are considered as the resilience enhancement strategies for TNS in this paper. In DNS, deployment of additional DGs can provide emergent power supply for distribution-level customers. To the further, MEG can flexibly facilitate power support with the spatial convenience. And the application of automatic switch can assist power distribution and maintain network topology under typhoons. Hence, these two measures along with line hardening are regarded as the resilience enhancement strategies for DNS in this work.

III. Model Formulation

The overall architecture of the resilience enhancement model via pre-event risk-based decentralized planning is shown in Fig. 3. The resilient TNS planning (RTNSP) problem and resilient DNS planning (RDNSP) problems are modeled independently with their active boundary power communicated through the boundary buses. The coordination between the RTNSP and RDNSP problems is achieved through decentralized identification of their corresponding interacted boundary power. The investment decisions include hardening and expansion of transmission network in TNS as well as distribution line hardening, MEG and automatic switch deployment in DNSs. The uncertainty of typhoon impact is modeled by the status of transmission/distribution lines in different typhoon scenarios. And the uncertainties of growth in load demand and RGC are captured in normal scenarios. To quantify the probabilistic risks brought by stochastic typhoons,

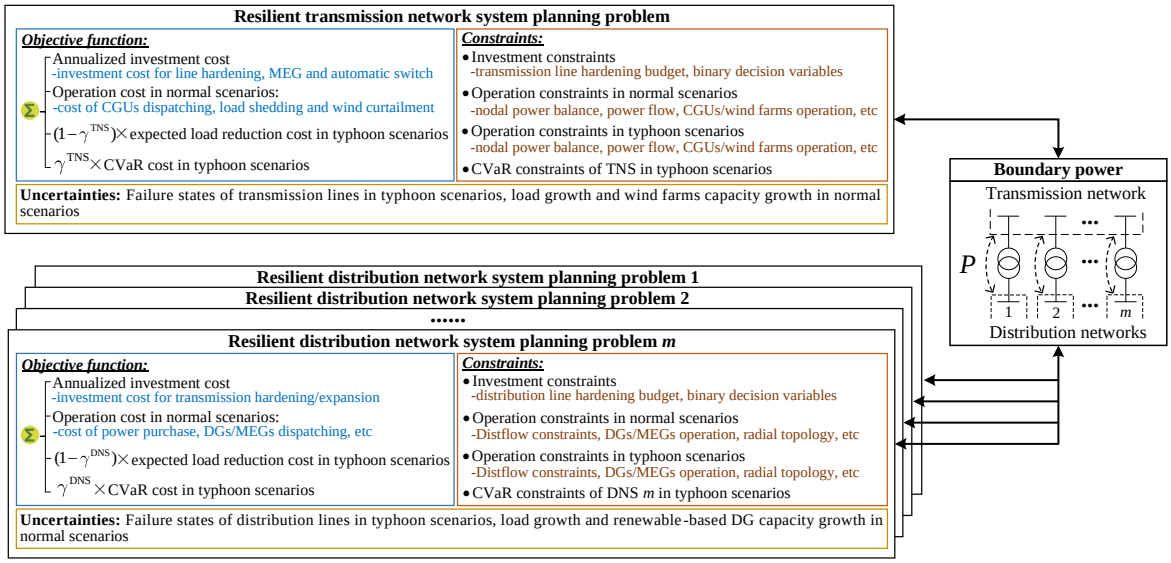

Fig. 3. Overall architecture of the risk-based decentralized planning model.

CVaR is introduced into the RTNSP and RDNSP problems. Wherein, γ^{TNS} and γ^{DNS} are the risk preference factors to adjust trade-off between risk-averse and risk-neutral decisions. Further details of the model are provided in the following.

A. Resilient TNS Planning (RTNSP) Problem

Firstly, we introduce the basic formulation of planning model. The goal of TNS planning problem is to minimize the investment cost, the expected operation cost under normal electricity growth scenarios as well as the expected load reduction cost and CVaR cost under typhoon disasters. The complete formulation of RTNSP problem is shown as follows.

$$\min\ C_{\mathrm{inv}}^{\mathrm{TNS}}+\sum_{s\in\mathcal{S}}\pi_s C_{\mathrm{ope},s}^{\mathrm{TNS}}+(1-\gamma^{\mathrm{TNS}})\sum_{s\in\mathcal{S}}\pi_s C^{\mathrm{ls,TNS}} r_{b,s}^{\mathrm{U,TNS}}\Delta^{\mathrm{du}} +\gamma^{\mathrm{TNS}} C^{\mathrm{ls,TNS}}\cdot \mathrm{CVaR}(\Psi_s^{\mathrm{TNS}},\delta)\cdot\Delta^{\mathrm{du}} \tag{2}$$

$$C_{\mathrm{inv}}^{\mathrm{TNS}}=C_{\mathrm{inv,ini}}^{\mathrm{TNS}}\cdot\frac{IR(1+IR)^{Y}}{(1+IR)^{Y}-1} \tag{3}$$

$$C_{\mathrm{inv,ini}}^{\mathrm{TNS}}=\sum_{l\in\Gamma^{\mathrm{TNS}}} C_l^{\mathrm{H,TNS}} x_l^{\mathrm{H,TNS}}+\sum_{l\in\Gamma^{\mathrm{TNS*}}} C_l^{\mathrm{L,TNS}} x_l^{\mathrm{L,TNS}} \tag{4}$$

$$C_{\mathrm{ope},s}^{\mathrm{TNS}}=\sum_{g\in\Omega_b^{\mathrm{TNS}}} C_g^{\mathrm{su,TNS}} SU_{g,s}\Delta^{\mathrm{du}}+\sum_{g\in\Omega^{\mathrm{TNS}}} C_g^{\mathrm{op,TNS}} P_{g,s}^{\mathrm{G}}\Delta^{\mathrm{du}} +\sum_{b\in\Xi^{\mathrm{TNS}}} C^{\mathrm{ls,TNS}} r_{b,s}^{\mathrm{U,TNS}}\Delta^{\mathrm{du}}+\sum_{w\in\Theta^{\mathrm{TNS}}} C^{\mathrm{wc,TNS}} r_{w,s}^{\mathrm{W,TNS}}\Delta^{\mathrm{du}} \tag{5}$$

subject to:

1) Investment constraints:

$$\sum_{l\in\Gamma^{\mathrm{TNS}}} C_l^{\mathrm{H,TNS}} x_l^{\mathrm{H,TNS}}\le\zeta^{\mathrm{H,TNS}} \tag{6}$$

$$x_l^{\mathrm{H,TNS}},x_l^{\mathrm{L,TNS}}\in\{0,1\}\quad\forall l \tag{7}$$

2) Operation constraints in normal and typhoon scenarios:

$$\sum_{\forall g\in\Omega_b^{\mathrm{TNS}}} P_{g,s}^{\mathrm{G}}+\sum_{\forall w\in\Theta^{\mathrm{TNS}}} P_{w,s}^{\mathrm{W}}+\sum_{\forall l\in(\Gamma_b^{\mathrm{TNS}}\cup\Gamma_b^{\mathrm{TNS*}})|\mathrm{re}(l)=b} f_{l,s} -\sum_{\forall l\in(\Gamma_b^{\mathrm{TNS}}\cup\Gamma_b^{\mathrm{TNS*}})|\mathrm{se}(l)=b} f_{l,s}=\kappa_s D_b^{\mathrm{TNS}}+\sum_{\forall m}\sum_{\forall o\in\Xi_b^{\mathrm{TD}}} P_{o,s,m}^{\mathrm{TD}}-r_{b,s}^{\mathrm{U,TNS}} \quad\forall b\in\Xi^{\mathrm{TNS}},\ \forall s\in\mathcal{S} \tag{8}$$

$$-(1-(x_l^{\mathrm{H,TNS}}+\xi_{l,s}^{\mathrm{TNS}}-\xi_{l,s}^{\mathrm{TNS}}x_l^{\mathrm{H,TNS}}))M\le f_{l,s}-B_l\cdot(\theta_{\mathrm{se}(l),s}-\theta_{\mathrm{re}(l),s}) \le(1-(x_l^{\mathrm{H,TNS}}+\xi_{l,s}^{\mathrm{TNS}}-\xi_{l,s}^{\mathrm{TNS}}x_l^{\mathrm{H,TNS}}))M\quad\forall l\in\Gamma^{\mathrm{TNS}},\ \forall s\in\mathcal{S} \tag{9}$$

$$-(x_l^{\mathrm{H,TNS}}+\xi_{l,s}^{\mathrm{TNS}}-\xi_{l,s}^{\mathrm{TNS}}x_l^{\mathrm{H,TNS}})F_l^{\max}\le f_{l,s} \le(x_l^{\mathrm{H,TNS}}+\xi_{l,s}^{\mathrm{TNS}}-\xi_{l,s}^{\mathrm{TNS}}x_l^{\mathrm{H,TNS}})F_l^{\max}\quad\forall l\in\Gamma^{\mathrm{TNS}},\ \forall s\in\mathcal{S} \tag{10}$$

$$-(1-x_l^{\mathrm{L,TNS}})M\le f_{l,s}-B_l(\theta_{\mathrm{se}(l),s}-\theta_{\mathrm{re}(l),s}) \le(1-x_l^{\mathrm{L,TNS}})M\quad\forall l\in\Gamma^{\mathrm{TNS*}},\ \forall s\in\mathcal{S} \tag{11}$$

$$-x_l^{\mathrm{L,TNS}}F_l^{\max}\le f_{l,s}\le x_l^{\mathrm{L,TNS}}F_l^{\max}\quad\forall l\in\Gamma^{\mathrm{TNS*}},\ \forall s\in\mathcal{S} \tag{12}$$

$$SU_{g,s}P_g^{\mathrm{G\,min}}\le P_{g,s}^{\mathrm{G}}\le SU_{g,s}P_g^{\mathrm{G\,max}}\quad\forall g\in\Omega^{\mathrm{TNS}},\ \forall s\in\mathcal{S} \tag{13}$$

$$P_{w,s}^{\mathrm{W}}+r_{w,s}^{\mathrm{W,TNS}}=c_w^{\mathrm{W,TNS}}\vartheta_s^{\mathrm{TNS}}P_w^{\mathrm{W\,max}}\quad\forall w\in\Theta^{\mathrm{TNS}},\ \forall s\in\mathcal{S} \tag{14}$$

$$0\le P_{w,s}^{\mathrm{W}}\le c_w^{\mathrm{W,TNS}}\vartheta_s^{\mathrm{TNS}}P_w^{\mathrm{W\,max}}\quad\forall w\in\Theta^{\mathrm{TNS}},\ \forall s\in\mathcal{S} \tag{15}$$

$$0\le r_{b,s}^{\mathrm{U,TNS}}\le\kappa_s D_b^{\mathrm{TNS}}\quad\forall b\in\Xi^{\mathrm{TNS}},\ \forall s\in\mathcal{S} \tag{16}$$

Eq.(2) represents the objective function of RTNSP problem. The total annualized investment cost comprises the cost of transmission expansion and line hardening, as in (3)-(4), which takes the interest rate IR and planning years Y into account. The expected total operation cost under normal scenarios in (5) incorporates the startup, operation cost of the conventional generating units (CGUs), shedding punishment cost of power load and curtailment cost of wind power. Eq.(17) indicates the load reduction in TNS under typhoon scenarios. Constraint (6) sets the investment budgets for line hardening. Constraint (7) defines the binary nature of investment decision variables. Eq.(8) ensures the nodal power balance of TNS. DC power flow of the existing transmission lines under the mutual impact of hardening and typhoons is modeled in (9), where a real number M with a big positive value is introduced for linearization. Constraint (10) imposes upper and lower bounds on power flow. Constraints (11)-(12) model the DC power flow and line transmission capacity of candidate transmission lines. Constraint (13) limits the power output of the CGUs. Constraints (14)-(15) characterize the power output range of wind farms. Constraint (16) expresses the range of unserved power load in TNS.

3) CVaR constraints in typhoon scenarios:

$$\Psi_s^{\mathrm{TNS}}=\sum_{b\in\Xi^{\mathrm{TNS}}} r_{b,s}^{\mathrm{U,TNS}}\quad\forall s\in\tilde{\mathcal{S}} \tag{17}$$

$$\Psi_s^{\mathrm{TNS}} - \mathrm{VaR}^{\mathrm{TNS}} - \sigma_s^{\mathrm{TNS}} \le 0 \quad \forall s \in \tilde{\mathcal{S}} \tag{18}$$

$$\sigma_s^{\mathrm{TNS}} \ge 0 \quad \forall s \in \tilde{\mathcal{S}} \tag{19}$$

$$\mathrm{CVaR}(\Psi_s^{\mathrm{TNS}}, \delta) = \mathrm{VaR}^{\mathrm{TNS}} + \frac{1}{1-\delta} \sum_{s \in \tilde{\mathcal{S}}} \pi_s \sigma_s^{\mathrm{TNS}} \tag{20}$$

where $\mathrm{CVaR}(\Psi_s^{\mathrm{TNS}}, \delta)$ represents the quantified load reduction risk in typhoon extreme scenarios for TNS. $\mathrm{VaR}^{\mathrm{TNS}}$ represents the expected load reduction in typhoon scenarios under confidence level δ. σ_s^{TNS} is the auxiliary variable in RTNSP.

B. Resilient DNS Planning (RDNSP) Problem

Similar to RTNSP, the objective of RDNSP problem is to minimize investment cost, the expected cost in normal scenarios as well as the expected load reduction cost and CVaR cost in typhoon disasters. The complete model of RDNSP for each DNS *m* is formulated in the following parts. For brief expression, the subscript *m* in each letter is omitted except the boundary variable.

$$\begin{aligned} \min \ & C_{\mathrm{inv}}^{\mathrm{DNS}} + \sum_{s \in \mathcal{S}} \pi_s C_{\mathrm{ope},s}^{\mathrm{DNS}} + (1-\gamma^{\mathrm{DNS}}) \sum_{s \in \mathcal{S}} \pi_s C^{\mathrm{ls,DNS}} r_{i,s}^{\mathrm{U,DNS}} \Delta^{\mathrm{du}} \\ & + \gamma^{\mathrm{DNS}} C^{\mathrm{ls,DNS}} \cdot \mathrm{CVaR}(\Psi_s^{\mathrm{DNS}}, \delta) \cdot \Delta^{\mathrm{du}} \end{aligned} \tag{21}$$

$$C_{\mathrm{inv}}^{\mathrm{DNS}} = C_{\mathrm{inv,ini}}^{\mathrm{DNS}} \cdot \frac{IR(1+IR)^Y}{(1+IR)^Y - 1} \tag{22}$$

$$C_{\mathrm{inv,ini}}^{\mathrm{DNS}} = \sum_{ij \in \Gamma^{\mathrm{DNS}}} C_{ij}^{\mathrm{H,DNS}} x_{ij}^{\mathrm{H,DNS}} + \sum_{k \in \Omega^{\mathrm{DNS+}}} C_k^{\mathrm{Ginv}} x_k^{\mathrm{MG}} + \sum_{ij \in \Gamma^{\mathrm{DNS}}} C_{ij}^{\mathrm{AS}} x_{ij}^{\mathrm{AS}} \tag{23}$$

$$\begin{aligned} C_{\mathrm{ope.s}}^{\mathrm{DNS}} = & \sum_{o \in \Xi_m^{\mathrm{DT}}} C_o^{\mathrm{buy,DNS}} P_{o,s,m}^{\mathrm{DT}} \Delta^{\mathrm{du}} \\ & + \sum_{i \in \Xi^{\mathrm{DNS}}} C^{\mathrm{op,DNS}} P_{i,s}^{\mathrm{CD}} \Delta^{\mathrm{du}} + \sum_{k \in \Omega^{\mathrm{DNS+}}} \sum_{i \in \Xi^{\mathrm{DNS}}} C^{\mathrm{om,DNS}} P_{i,k,s}^{\mathrm{MG}} \Delta^{\mathrm{du}} \\ & + \sum_{i \in \Xi^{\mathrm{DNS}}} C^{\mathrm{ls,DNS}} r_{i,s}^{\mathrm{U,DNS}} \Delta^{\mathrm{du}} + \sum_{i \in \Xi^{\mathrm{DNS}}} C^{\mathrm{wc,DNS}} r_{i,s}^{\mathrm{WD,DNS}} \Delta^{\mathrm{du}} \end{aligned} \tag{24}$$

subject to:

1) Investment constraints:

$$\sum_{ij \in \Gamma^{\mathrm{DNS}}} C_{ij}^{\mathrm{H,DNS}} x_{ij}^{\mathrm{H,DNS}} \le \zeta^{\mathrm{H,DNS}} \tag{25}$$

$$x_{ij}^{\mathrm{H,DNS}}, x_k^{\mathrm{MEG}}, x_{ij}^{\mathrm{AS}} \in \{0,1\} \quad \forall ij, \ \forall k \tag{26}$$

2) Operation constraints in normal and typhoon scenarios:

$$\begin{aligned} & \sum_{\forall ij \in \Gamma^{\mathrm{DNS}}} (p_{ij,s} - L_{ij,s} R_{ij}) + P_{j,s}^{\mathrm{CD}} + P_{j,s}^{\mathrm{WD}} + P_{j,k,s}^{\mathrm{MG}} + \sum_{\forall o \in \Xi_{j,m}^{DT}} P_{o,s,m}^{\mathrm{DT}} \\ & = \kappa_s D_j^{\mathrm{DNS}} - r_{j,s,}^{\mathrm{U,DNS}} \ \forall j \in \Xi^{\mathrm{DNS}}, \ \forall k \in \Omega^{\mathrm{DNS+}}, \ \forall s \in \mathcal{S} \end{aligned} \tag{27}$$

$$\begin{aligned} & \sum_{\forall ij \in \Gamma^{\mathrm{DNS}}} (q_{ij,s} - L_{ij,s} X_{ij}) + Q_{j,s}^{\mathrm{CD}} + Q_{j,s}^{\mathrm{WD}} + Q_{j,k,s}^{\mathrm{MG}} \\ & + \sum_{\forall o \in \Xi_{j,m}^{DT}} Q_{o,s,m}^{\mathrm{DT}} = Q_j^{\mathrm{DNS}} \quad \forall j \in \Xi^{\mathrm{DNS}}, \ \forall k \in \Omega^{\mathrm{DNS+}}, \ \forall s \in \mathcal{S} \end{aligned} \tag{28}$$

$$\begin{cases} U_{i,s} \ge -(1-\alpha_{ij,s}) \cdot M + U_{j,s} - 2(R_{ij} p_{ij,s} + X_{ij} q_{ij,s}) - (R_{ij}^2 + X_{ij}^2) L_{ij,s} \\ U_{i,s} \le (1-\alpha_{ij,s}) \cdot M + U_{j,s} - 2(R_{ij} p_{ij,s} + X_{ij} q_{ij,s}) - (R_{ij}^2 + X_{ij}^2) L_{ij,s} \end{cases} \tag{29}$$
$$\forall ij \in \Gamma^{\mathrm{DNS}}, \ \forall s \in \mathcal{S}$$

$$\left\| 2p_{ij,s} \ \ 2q_{ij,s} \ \ L_{ij,s} - U_{j,s} \right\|_2 \le L_{ij,s} + U_{j,s} \tag{30}$$
$$\forall ij \in \Gamma^{\mathrm{DNS}}, \ \forall j \in \Xi^{\mathrm{DNS}}, \ \forall s \in \mathcal{S}$$

$$Q_{o,s,m}^{\mathrm{DT}} = P_{o,s,m}^{\mathrm{DT}} \tan \arccos \phi_o \quad \forall o \in \Xi_m^{\mathrm{DT}}, \ \forall s \in \mathcal{S}, \ \forall m \tag{31}$$

$$\alpha_{ij,s} \cdot (I_{ij}^{\min})^2 \le L_{ij,s} \le \alpha_{ij,s} \cdot (I_{ij}^{\max})^2 \quad \forall ij \in \Gamma^{\mathrm{DNS}}, \ \forall s \in \mathcal{S} \tag{32}$$

$$(V_i^{\min})^2 \le U_{i,s} \le (V_i^{\max})^2 \quad \forall i \in \Xi^{\mathrm{DNS}}, \ \forall s \in \mathcal{S} \tag{33}$$

$$-\alpha_{ij,s} \cdot M \le p_{ij,s}, q_{ij,s} \le \alpha_{ij,s} \cdot M \quad \forall ij \in \Gamma^{\mathrm{DNS}}, \ \forall s \in \mathcal{S} \tag{34}$$

$$P_i^{\mathrm{CD\,min}} \le P_{i,s}^{\mathrm{CD}} \le P_i^{\mathrm{CD\,max}} \quad \forall i, \ \forall s \in \mathcal{S}, \tag{35}$$

$$Q_i^{\mathrm{CD\,min}} \le Q_{i,s}^{\mathrm{CD}} \le Q_i^{\mathrm{CD\,max}} \quad \forall i, \ \forall s \in \mathcal{S} \tag{36}$$

$$P_{i,s}^{\mathrm{WD}} + r_{i,s}^{\mathrm{WD,DNS}} = c^{\mathrm{WD,DNS}} \vartheta_s^{\mathrm{DNS}} P_i^{\mathrm{WD\,max}} \quad \forall i, \ \forall s \in \mathcal{S} \tag{37}$$

$$0 \le P_{i,s}^{\mathrm{WD}} \le c^{\mathrm{WD,DNS}} \vartheta_s^{\mathrm{DNS}} P_i^{\mathrm{WD\,max}} \quad \forall i, \ \forall s \in \mathcal{S} \tag{38}$$

$$Q_{i,s}^{\mathrm{WD}} = P_{i,s}^{\mathrm{WD}} \tan \arccos \phi_i^{\mathrm{WD}} \quad \forall i, \ \forall s \in \mathcal{S} \tag{39}$$

$$\begin{aligned} & \varphi_{i,k,s} P_k^{\mathrm{MG\,min}} \le P_{i,k,s}^{\mathrm{MG}} \le \varphi_{i,k,s} P_k^{\mathrm{MG\,max}} \\ & \forall i, \ \forall k \in \Omega^{\mathrm{DNS+}}, \ \forall s \in \mathcal{S} \end{aligned} \tag{40}$$

$$\begin{aligned} & \varphi_{i,k,s} Q_k^{\mathrm{MG\,min}} \le Q_{i,k,s}^{\mathrm{MG}} \le \varphi_{i,k,s} Q_{k,}^{\mathrm{MG\,max}} \\ & \forall i, \ \forall k \in \Omega^{\mathrm{DNS+}}, \ \forall s \in \mathcal{S} \end{aligned} \tag{41}$$

$$\sum_i \varphi_{i,k,s} \le x_k^{\mathrm{MG}} \quad \forall i, \ \forall k \in \Omega^{\mathrm{DNS+}}, \ \forall s \in \mathcal{S} \tag{42}$$

$$0 \le r_{i,s}^{\mathrm{U,DNS}} \le \kappa_s D_{i,}^{\mathrm{DNS}} \ \forall i \in \Xi^{\mathrm{DNS}}, \forall s \in \mathcal{S} \tag{43}$$

$$\sum_{ij \in \Gamma^{\mathrm{DNS}}} \alpha_{ij,s} = \mathrm{card}(\Xi^{\mathrm{DNS}}) - 1 \quad \forall s \in \mathcal{S}, \tag{44}$$

$$\beta_{ji,s} + \beta_{ij,s} = \alpha_{ij,s} \quad \forall ij \in \Gamma^{\mathrm{DNS}}, \ \forall s \in \mathcal{S} \tag{45}$$

$$\sum_i \beta_{ji,s} = 1 \quad \forall j \in \Xi^{\mathrm{DNS}}, \ \forall s \in \mathcal{S} \tag{46}$$

$$\alpha_{ij,s,m} \le x_{ij}^{\mathrm{H,DNS}} + \xi_{ij,s}^{\mathrm{DNS}} - \xi_{ij,s}^{\mathrm{DNS}} x_{ij,}^{\mathrm{H,DNS}} \quad \forall ij \in \Gamma^{\mathrm{DNS}}, \ \forall s \in \mathcal{S} \tag{47}$$

$$\begin{aligned} \alpha_{ij,s} \ge & x_{ij}^{\mathrm{H,DNS}} + \xi_{ij,s}^{\mathrm{DNS}} - \xi_{ij,s}^{\mathrm{DNS}} x_{ij}^{\mathrm{H,DNS}} - x_{ij}^{\mathrm{AS}} - \tau_{ij} \\ & \forall ij \in \Gamma^{\mathrm{DNS}}, \ \forall s \in \mathcal{S} \end{aligned} \tag{48}$$

Eq.(21) represents the objective function of RDNSP. The total annualized investment cost includes three terms related with hardening distribution line, MEG deployment and automatic switch installation, as shown in (22)-(24). Eq.(24) formulates the expected operation cost under normal scenarios, which includes the cost of power purchase from TNS, the operation cost of DG and MEG, the punishment cost for unserved load power and renewable curtailment. Eq.(49) indicates the load reduction in DNS under typhoon scenarios. Constraint (25) imposes the investment budgets on line hardening. Constraint (26) defines the binary status of investment decision variables. The DistFlow model incorporating power balance, branch flow and second-order cone constraint is defined in (27)-(30) which is linearized by big-M method [43]. Constraint (31) indicates the calculation of reactive exchange power $Q_{o,s,m}^{\mathrm{DT}}$ of CTDS with power factor. Constraints (32)-(33) set the upper and lower limit on current and voltage magnitude. Constraint (34) regulates the power flow passing through each branch which is decided by its line status. Constraints (35)-(36) state the bounds for power output of traditional DGs. Constraints (37)-(39) introduce the power output model of renewable-based DGs. Constraints (40)-(41) express the power output of MEGs. Constraint (42) ensures the location variable of MEG is decided by its investment decision variable. Constraint (43) sets the boundary of

unserved power load in DNS. Constraints (44)-(46) preserve the radial topology of distribution network. Card(·) represents the number of elements in a set. Constraint (47) represents the reconfiguration status of distribution lines under the mutual impact of hardening and typhoons. Constraint (48) expresses the status of distribution lines considering the extra impact of the installing automatic switches and tie-line characteristic in addition to the influence of hardening and typhoons.

3) CVaR constraints in typhoon scenarios:

$$\Psi_s^{\mathrm{DNS}} = \sum_{i\in\Xi^{\mathrm{DNS}}} r_{i,s}^{\mathrm{U,DNS}} \quad \forall s \in \tilde{\mathcal{S}} \tag{49}$$

$$\Psi_s^{\mathrm{DNS}} - \mathrm{VaR}^{\mathrm{DNS}} - \sigma_s^{\mathrm{DNS}} \le 0 \quad \forall s \in \tilde{\mathcal{S}} \tag{50}$$

$$\sigma_s^{\mathrm{DNS}} \ge 0 \quad \forall s \in \tilde{\mathcal{S}} \tag{51}$$

$$\mathrm{CVaR}(\Psi_s^{\mathrm{DNS}}, \delta) = \mathrm{VaR}^{\mathrm{DNS}} + \frac{1}{1-\delta}\sum_{s\in\tilde{\mathcal{S}}} \pi_s \sigma_s^{\mathrm{DNS}} \tag{52}$$

where $\mathrm{CVaR}(\Psi_s^{\mathrm{DNS}}, \delta)$ represents the quantified load reduction risk in typhoon extreme scenarios for DNS. $\mathrm{VaR}^{\mathrm{DNS}}$ represents the expected load reduction in extreme scenarios under confidence level δ. σ_s^{DNS} is the auxiliary variable in RDNSP.

IV. Solution Methodology

In this section, an integrated iterative solution process is designed for solving the proposed planning model. In section IV-A, the model reformulation is prepared for ADMM which can achieve a fully decentralized manner. In section IV-B, an improved PHA with scenario bundling is introduced for accelerating the collaborative computation of multi-scenario problems representing uncertainties. In section IV-C, the solution procedure of the integrated algorithm is presented.

A. Model reformulation for implementing ADMM

The ADMM is employed for the interaction of power information between TNS and DNSs, thereby ensuring data privacy and decision-making independency of each system. For ADMM, the RTNSP and RDNSP models are reformulated with their Lagrangian functions, which are abbreviated below.

Reformulated RTNSP model:

$$\begin{aligned}\min\ & \boldsymbol{C}^{\mathrm{T}}\boldsymbol{x}^{\mathrm{TNS}} + \sum_{s\in\tilde{\mathcal{S}}}\pi_s \boldsymbol{H}^{\mathrm{T}}\boldsymbol{y}_s + (1-\gamma^{\mathrm{TNS}})\sum_{s\in\tilde{\mathcal{S}}}\pi_s C^{\mathrm{ls,TNS}} r_{b,s}^{\mathrm{U,TNS}}\Delta^{\mathrm{du}} \\ & + \gamma^{\mathrm{TNS}} C^{\mathrm{ls,TNS}}\mathrm{CVaR}^{\mathrm{TNS}}\Delta^{\mathrm{du}} + \mathfrak{L}^{\mathrm{TNS}}\end{aligned} \tag{53}$$

$$s.t. \quad \boldsymbol{A}\boldsymbol{x}^{\mathrm{TNS}} \le \boldsymbol{c},\ \boldsymbol{x}^{\mathrm{TNS}} \in \{0,1\},\ \boldsymbol{F}\boldsymbol{y}_s \le \boldsymbol{D} - \boldsymbol{e}\boldsymbol{x}^{\mathrm{TNS}} \tag{54}$$

Reformulated RDNSP model:

$$\begin{aligned}\min\ & \boldsymbol{Q}^{\mathrm{T}}\boldsymbol{x}_m^{\mathrm{DNS}} + \sum_{s\in\tilde{\mathcal{S}}}\pi_s \boldsymbol{G}^{\mathrm{T}}\boldsymbol{z}_{s,m} + (1-\gamma_m^{\mathrm{DNS}})\sum_{s\in\tilde{\mathcal{S}}}\pi_s C^{\mathrm{ls,DNS}} r_{i,s,m}^{\mathrm{U,DNS}}\Delta^{\mathrm{du}} \\ & + \gamma_m^{\mathrm{DNS}} C^{\mathrm{ls,DNS}}\mathrm{CVaR}_m^{\mathrm{DNS}}\Delta^{\mathrm{du}} + \mathfrak{L}_m^{\mathrm{DNS}}\end{aligned} \tag{55}$$

$$s.t. \quad \boldsymbol{B}\boldsymbol{x}_m^{\mathrm{DNS}} \le \boldsymbol{h},\ \boldsymbol{x}_m^{\mathrm{DNS}} \in \{0,1\},\ \boldsymbol{L}\boldsymbol{z}_{s,m} \le \boldsymbol{J} - \boldsymbol{v}\boldsymbol{x}_m^{\mathrm{DNS}} \tag{56}$$

where $\boldsymbol{x}^{\mathrm{TNS}}$ and $\boldsymbol{x}_m^{\mathrm{DNS}}$ are the investment decision variables of TNS and DNS *m* respectively. $\boldsymbol{y}_s$ and $\boldsymbol{z}_{s,m}$ are the operation variables of TNS and DNS *m* respectively. $\boldsymbol{C}$, $\boldsymbol{H}$, $\boldsymbol{Q}$ and $\boldsymbol{G}$ are the cost coefficient vectors. $\boldsymbol{A}$, $\boldsymbol{F}$, $\boldsymbol{c}$, $\boldsymbol{D}$, $\boldsymbol{e}$ are the constant coefficient vectors related to the constraints of RTNSP problem. And $\boldsymbol{B}$, $\boldsymbol{L}$, $\boldsymbol{h}$, $\boldsymbol{J}$, $\boldsymbol{v}$ are the constant coefficient vectors related to the constraints of RDNSP problem. Constraint (54) represents the formulation (6)-(16) of RTNSP problem. Constraint (56) represents the formulation (25)-(48) of RDNSP problem. $\mathfrak{L}^{\mathrm{TNS}}$ and $\mathfrak{L}_m^{\mathrm{DNS}}$ are the Lagrangian functions of TNS and DNS *m* respectively, which are shown below.

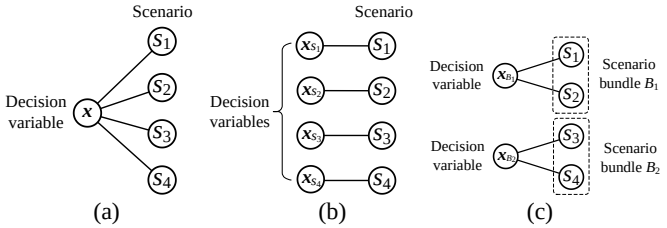

Fig. 4. Comparison of the (a) original problem, (b) PHA-based decomposed subproblems and (c) BPHA-based decomposed subproblems with 4 scenarios.

$$\mathfrak{L}_d^{\mathrm{TNS}} = \sum_m \Big(\sum_s \pi_s \sum_{o\in\Xi^{\mathrm{TD}}} \big(\lambda_{o,s,m}^{\mathrm{TNS}}(P_{o,s,m}^{\mathrm{TD}} - \bar{P}_{o,s,m}) + \frac{\rho_{o,s,m}^{\mathrm{TNS}}}{2}\left\|P_{o,s,m}^{\mathrm{TD}} - \bar{P}_{o,s,m}\right\|_2^2\big)\Big) \tag{57}$$

$$\mathfrak{L}_{d,m}^{\mathrm{DNS}} = \sum_s \pi_s \sum_{o\in\Xi^{\mathrm{DT}(m)}} \big(\lambda_{o,s,m}^{\mathrm{DNS}}(P_{o,s,m}^{\mathrm{DT}} - \bar{P}_{o,s,m}) + \frac{\rho_{o,s,m}^{\mathrm{DNS}}}{2}\left\|P_{o,s,m}^{\mathrm{DT}} - \bar{P}_{o,s,m}\right\|_2^2\big) \tag{58}$$

where $\lambda_{o,s,m}^{\mathrm{TNS}}$ and $\lambda_{o,s,m}^{\mathrm{DNS}}$ are the multiplier parameters of ADMM. $\rho_{o,s,m}^{\mathrm{TNS}}$ and $\rho_{o,s,m}^{\mathrm{DNS}}$ are the penalty parameters of ADMM. $\bar{P}_{o,s,m}$ is the global boundary variable between TNS and DNS *m* which is calculated as $\bar{P}_{o,s,m} = (P_{o,s,m}^{\mathrm{TD}} + P_{o,s,m}^{\mathrm{DT}})/2$. To date, the model reformulation for conducting ADMM has been complete and a detailed procedure for specific ADMM will be presented in section IV-C.

B. Principle of BPHA with scenario bundling

In consideration of the stochastic mixed integer planning problem with multiple scenarios, PHA is often employed to tackle the resolution by decomposing the problem into single-scenario subproblems, where each investment decision variable corresponds to each single scenario [44]. To this further, a bundle-based PHA is customized to establish the main framework for solving the decentralized multi-scenario planning problem. Its peculiarity lies in its capability to encapsulate a subset of scenarios within a scenario bundle for planning, where each generated decision variable corresponds to each scenario bundle. The improvement principle of such BPHA is illustrated in Fig. 4. Compared to PHA, the BPHA with scenario bundling can enhance the quality of PHA's lower bounds and accelerate the iteration speed of this algorithm [19], [45]. By selecting an appropriate number of scenarios in each bundle, the frequency of solving processes during PHA iteration is reduced, leading to computational time savings and accuracy enhancement.

By differentiating the combination of normal scenarios and typhoon scenarios in a scenario bundle, the scenarios in each bundle can be determined. And the attached probability can be identified as $\pi_d = \sum_{s\in\mathcal{S}_d}\pi_s,\ d\in\mathcal{B}$, wherein π_d is the probability of scenario bundle *d*, $\mathcal{S}_d$ represents the set of scenarios in scenario bundle *d*.

Algorithm 1: ADMM for an individual-bundle problem.

Initialization: Set the initial value of $\bar{P}_{o,s,m}$, $\lambda_{o,s,m}^{\mathrm{TNS}}$, $\lambda_{o,s,m}^{\mathrm{DNS}}$, $\rho_{o,s,m}^{\mathrm{TNS}}$ and $\rho_{o,s,m}^{\mathrm{DNS}}$; Set the residual tolerances $\varepsilon_1, \varepsilon_2$

Iteration:

for n = 1, 2, …, **do**

Solve the selected RTNSP problem to obtain $P_{o,s,m}^{\mathrm{TD},(n)}$

Solve the selected RDNSP problem to obtain $P_{o,s,m}^{\mathrm{DT},(n)}$

Update global variable: $\bar{P}_{o,s,m}^{(n)} = (P_{o,s,m}^{\mathrm{TD},(n)} + P_{o,s,m}^{\mathrm{DT},(n)})/2$

Update the multiplier parameters based on (59)

$$\begin{cases} \lambda_{o,s,m}^{\mathrm{TNS},(n+1)} = \lambda_{o,s,m}^{\mathrm{TNS},(n)} + \rho_{o,s,m}^{\mathrm{TNS},(n)}(P_{o,s,m}^{\mathrm{TD},(n)} - \bar{P}_{o,s,m}^{(n)}) \\ \lambda_{o,s,m}^{\mathrm{DNS},(n+1)} = \lambda_{o,s,m}^{\mathrm{DNS},(n)} + \rho_{o,s,m}^{\mathrm{DNS},(n)}(P_{o,s,m}^{\mathrm{DT},(n)} - \bar{P}_{o,s,m}^{(n)}) \end{cases} \tag{59}$$

Calculate the residuals R_1 and R_2 of updated boundary power vectors based on (60)

$$\begin{cases} R_1 = \max_s(\left\| \boldsymbol{P}_s^{\mathrm{TD},(n)} - \bar{\boldsymbol{P}}_s^{(n+1)} \right\|_2) \\ R_2 = \max_s(\left\| \bar{\boldsymbol{P}}_s^{(n+1)} - \bar{\boldsymbol{P}}_s^{(n)} \right\|_2) \end{cases} \tag{60}$$

if $R_1 \le \varepsilon_1$, $R_2 \le \varepsilon_2$ **then** Stop

else

Update the penalty parameters of ADMM based on (A1)-(A2), which accelerates the convergency [51]

end if

$n \leftarrow n + 1$

end for

Output: Record the value of $\boldsymbol{x}_d^{\mathrm{TNS}}$, $\boldsymbol{x}_{d,m}^{\mathrm{DNS}}$, $\boldsymbol{y}_d$ and $\boldsymbol{z}_{d,m}$

C. Iterative process of the BPHA integrated with ADMM

In the iterative solution framework, ADMM is employed for the coordination of active power information exchange between TNS and DNSs in each bundle within each iteration of BPHA. To this end, the ADMM procedure for an individual-bundle problem embedded into the BPHA process is introduced firstly, which is described in **Algorithm 1**.

To implement complete BPHA, the objective functions of reformulated RTNSP and RDNSP models are extended with the introduction of $\boldsymbol{\omega}_d^{\mathrm{TNS},(u)}$, $\boldsymbol{\omega}_{d,m}^{\mathrm{DNS},(u)}$ and $\boldsymbol{\mu}^{\mathrm{TNS},(u)}$, $\boldsymbol{\mu}_m^{\mathrm{DNS},(u)}$ to enforce the non-anticipativity policy for all scenario bundles [19], which are shown below.

Extended RTNSP model:

$$\begin{aligned} \min\ & \boldsymbol{C}^{\mathrm{T}}\boldsymbol{x}_d^{\mathrm{TNS}} + \sum_{s\in\bar{\mathcal{S}}_d}\pi_s\boldsymbol{H}^{\mathrm{T}}\boldsymbol{y}_{s,d} + (1-\gamma^{\mathrm{TNS}})\sum_{s\in\mathcal{S}}\pi_s C^{\mathrm{ls,DNS}} r_{i,s}^{\mathrm{U,DNS}}\Delta^{\mathrm{du}} \\ & + \gamma^{\mathrm{TNS}} C^{\mathrm{ls,TNS}}\mathrm{CVaR}^{\mathrm{TNS}}\Delta^{\mathrm{du}} + \mathfrak{L}_d^{\mathrm{TNS}} \\ & + \boldsymbol{\omega}_d^{\mathrm{TNS},(u)}\boldsymbol{x}_d^{\mathrm{TNS}} + \frac{\boldsymbol{\mu}^{\mathrm{TNS},(u)}}{2}\left\| \boldsymbol{x}_d^{\mathrm{TNS}} - \bar{\boldsymbol{x}}^{\mathrm{TNS}} \right\| \end{aligned} \tag{61}$$

$$s.t.\quad \boldsymbol{A}\boldsymbol{x}_d^{\mathrm{TNS}} \le \boldsymbol{c},\ \boldsymbol{x}_d^{\mathrm{TNS}} \in \{0,1\},\ \boldsymbol{F}\boldsymbol{y}_{s,d} \le \boldsymbol{D} - \boldsymbol{e}\boldsymbol{x}_d^{\mathrm{TNS}} \tag{62}$$

Extended RDNSP model:

$$\begin{aligned} \min\ & \boldsymbol{Q}^{\mathrm{T}}\boldsymbol{x}_{d,m}^{\mathrm{DNS}} + \sum_{s\in\bar{\mathcal{S}}_d}\pi_s\boldsymbol{G}^{\mathrm{T}}\boldsymbol{z}_{s,d,m} + (1-\gamma_m^{\mathrm{DNS}})\sum_{s\in\bar{\mathcal{S}}_d}\pi_s C^{\mathrm{ls,DNS}} r_{i,s,m}^{\mathrm{U,DNS}}\Delta^{\mathrm{du}} \\ & + \gamma_m^{\mathrm{DNS}} C^{\mathrm{ls,DNS}}\mathrm{CVaR}_m^{\mathrm{DNS}}\Delta^{\mathrm{du}} + \mathfrak{L}_{d,m}^{\mathrm{DNS}} \\ & + \boldsymbol{\omega}_{d,m}^{\mathrm{DNS},(u)}\boldsymbol{x}_{d,m}^{\mathrm{DNS}} + \frac{\boldsymbol{\mu}_m^{\mathrm{DNS},(u)}}{2}\left\| \boldsymbol{x}_{d,m}^{\mathrm{DNS}} - \bar{\boldsymbol{x}}_{d,m}^{\mathrm{DNS}} \right\| \end{aligned} \tag{63}$$

$$s.t.\quad \boldsymbol{B}\boldsymbol{x}_{d,m}^{\mathrm{DNS}} \le \boldsymbol{h},\ \boldsymbol{x}_{d,m}^{\mathrm{DNS}} \in \{0,1\},\ \boldsymbol{L}\boldsymbol{z}_{s,d,m} \le \boldsymbol{J} - \boldsymbol{v}\boldsymbol{x}_{d,m}^{\mathrm{DNS}} \tag{64}$$

Algorithm 2: BPHA integrated with ADMM.

Initialization: Set the initial value of $\boldsymbol{\omega}_d^{\mathrm{TNS}}$, $\boldsymbol{\omega}_{d,m}^{\mathrm{DNS}}$ as 0 and $\boldsymbol{\mu}^{\mathrm{TNS}}$, $\boldsymbol{\mu}_m^{\mathrm{DNS}}$; Set the convergency thresholds $\varepsilon^{\mathrm{BPHA}}$

Selection: Identify (53)-(54) and (55)-(56) as the RTNSP and RDNSP problems to be solved in **Algorithm 1**

Iteration:

for each scenario bundle $d \in \mathcal{B}$ **do**

Implement the ADMM in **Algorithm 1** to obtain $\boldsymbol{x}_d^{\mathrm{TNS},(0)}$ and $\boldsymbol{x}_{d,m}^{\mathrm{DNS},(0)}$

end for

Aggregation: Calculate the respective aggregated vector: $\bar{\boldsymbol{x}}^{\mathrm{TNS},(0)} = \sum_{d=1}^{\mathrm{card}(\mathcal{B})}\pi_d\boldsymbol{x}_d^{\mathrm{TNS},(0)}$, $\bar{\boldsymbol{x}}_m^{\mathrm{DNS},(0)} = \sum_{d=1}^{\mathrm{card}(\mathcal{B})}\pi_d\boldsymbol{x}_{d,m}^{\mathrm{DNS},(0)}$

Selection: Identify (61)-(62) and (63)-(64) as the RTNSP and RDNSP problems to be solved in **Algorithm 1**

Iteration:

for u = 1, 2, …, **do**

Update the multipliers based on (65) and (66)

$$\boldsymbol{\omega}_d^{\mathrm{TNS},(u)} = \boldsymbol{\omega}_d^{\mathrm{TNS},(u-1)} + \boldsymbol{\mu}^{\mathrm{TNS},(u-1)}(\boldsymbol{x}_d^{\mathrm{TNS},(u-1)} - \bar{\boldsymbol{x}}^{\mathrm{TNS},(u-1)})\ \ \forall d \tag{65}$$

$$\boldsymbol{\omega}_{d,m}^{\mathrm{DNS},(u)} = \boldsymbol{\omega}_{d,m}^{\mathrm{DNS},(u-1)} + \boldsymbol{\mu}_m^{\mathrm{DNS},(u-1)}(\boldsymbol{x}_{d,m}^{\mathrm{DNS},(u-1)} - \bar{\boldsymbol{x}}_m^{\mathrm{DNS},(u-1)})\ \ \forall d \tag{66}$$

Iteration:

for each scenario bundle $d \in \mathcal{B}$ **do**

Implement **Algorithm 1** to obtain $\boldsymbol{x}_d^{\mathrm{TNS},(u)}$ and $\boldsymbol{x}_{d,m}^{\mathrm{DNS},(u)}$

end for

Aggregation: Calculate the respective aggregated vector: $\bar{\boldsymbol{x}}^{\mathrm{TNS},(u)} = \sum_{d=1}^{\mathrm{card}(\mathcal{B})}\pi_d\boldsymbol{x}_d^{\mathrm{TNS},(u)}$, $\bar{\boldsymbol{x}}_m^{\mathrm{DNS},(u)} = \sum_{d=1}^{\mathrm{card}(\mathcal{B})}\pi_d\boldsymbol{x}_{d,m}^{\mathrm{DNS},(u)}$

Aggregation: Group the decision vectors in both the TNS and DNSs based on (67) and (68)

$$\boldsymbol{x}_d^{(u)} = [(\boldsymbol{x}_d^{\mathrm{TNS},(u)})^{\mathrm{T}}, (\boldsymbol{x}_{d,1}^{\mathrm{DNS},(u)})^{\mathrm{T}}, ..., (\boldsymbol{x}_{d,m}^{\mathrm{DNS},(u)})^{\mathrm{T}}]^{\mathrm{T}} \tag{67}$$

$$\bar{\boldsymbol{x}}^{(u)} = [(\bar{\boldsymbol{x}}^{\mathrm{TNS},(u)})^{\mathrm{T}}, (\bar{\boldsymbol{x}}_1^{\mathrm{DNS},(u)})^{\mathrm{T}}, ..., (\bar{\boldsymbol{x}}_m^{\mathrm{DNS},(u)})^{\mathrm{T}}]^{\mathrm{T}} \tag{68}$$

if $\sum_{d=1}^{\mathrm{card}(\mathcal{B})}\pi_d\left\| \boldsymbol{x}_d^{(u)} - \bar{\boldsymbol{x}}^{(u)} \right\|^2 \le \varepsilon^{\mathrm{BPHA}}$ **then** Stop

else

update the penalty parameters based on (69) [46].

$$\boldsymbol{\mu}^{\mathrm{sys},(u+1)} = \boldsymbol{\mu}^{\mathrm{sys},(u)} \cdot \left\{ \chi \times \sum_{d\in\mathcal{B}} \left(\pi_d \left(\frac{\left\| \boldsymbol{x}_d^{\mathrm{sys},(u)} - \bar{\boldsymbol{x}}^{\mathrm{sys},(u)} \right\|^2}{\max \boldsymbol{x}_d^{\mathrm{sys},(u)} - \min \boldsymbol{x}_d^{\mathrm{sys},(u)} + 1} \right) \right) + 1 \right\} \tag{69}$$

where superscript *sys* represents the TNS or DNS. χ is the adjustment factor

end if

$u \leftarrow u + 1$

end for

Output: Final value of the $\boldsymbol{x}_d^{\mathrm{TNS},(u)}$, $\boldsymbol{x}_{d,m}^{\mathrm{DNS},(u)}$, $\boldsymbol{y}_{s,d}^{(u)}$ and $\boldsymbol{z}_{s,d,m}^{(u)}$

By incorporating the above-mentioned ADMM procedures into the BPHA framework with selected RTNSP and RDNSP problems to be solved, the overall programming problem can be solved systematically via the off-the-shelf commercial solver like Gurobi. After dividing the original scenarios into several scenario bundles, the whole iterative process of the solution methodology is described in **Algorithm 2**.

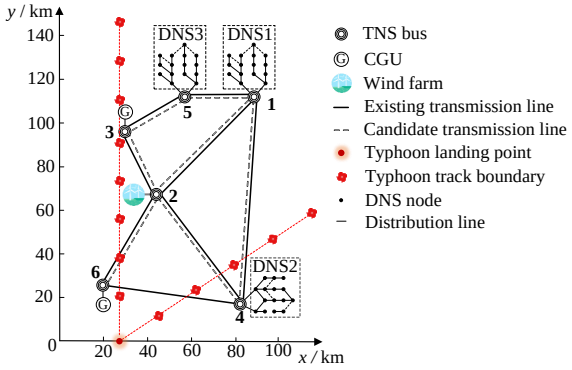

Fig. 5. Wiring and location schematic diagram of T6D3 system.

V. Case Studies

In this section, numerical experiments are performed on a T6D3 system and a T118D7 system which validate the effectiveness of the proposed method. Typhoon physical process in the CTDS is simulated by Batts model. All modeling and simulations are compiled in YALMIP run by MATLAB and the programming problems are solved by Gurobi on a computer with 2.50 GHz CPU and 16 GB RAM.

A. T6D3 Test System

The geographic wiring diagram of T6D3 test system is shown in Fig. 6. The system comprises one transmission network and three distribution networks which are located at bus 1, 4 and bus 5. In TNS, total power demand is 570 MW. Two CGUs are located at bus 3 and bus 6 with a capacity of 145 MW and 345 MW. The newly constructed transmission lines are assumed to possess sufficient strength to withstand the impact of typhoons without any adverse effects. The distance of the transmission corridor between each bus can be viewed in [47]. One wind farm with 210 MW is located at bus 2. The hardening and investment cost for each transmission line is set as 400 and 1000 $/(km·MW) [48]. Besides, the punishment cost for load shedding and wind power curtailment is set as 2000 $/MW and 200 $/MW. Investment budget for line hardening in TNS takes 1.4 M$. The boundaries of the possible typhoon's tracks are also displayed in Fig. 5. To represent the uncertainty of typhoons, eight typhoon tracks are generated by Monte Carlo simulation between the boundaries. The corresponding line failure rate and extreme line failure scenarios can be obtained by Batts model and sampling with threshold [49]. Besides, 4 scenarios are selected as normal scenarios for the uncertainties of load growth in CTDS, growth of wind farm capacity in TNS and growth of wind-based DG in DNS. To this end, 12 scenarios in total are formulated consisting of 4 normal and 8 typhoon scenarios. The probability ratio between normal scenarios and extreme scenarios is set as 9:1. And CVaR metric is applied to capture the tail risk of typhoon scenarios.

The schematic diagram of three distribution networks as DNS1, DNS2 and DNS3 are shown in Fig. 6. The capacity of conventional DGs and wind-based DGs in three DNSs are 8 MW and 5 MW. Each DNS can deploy two candidate MEGs with a capacity of 5 MW at the access nodes. The topology

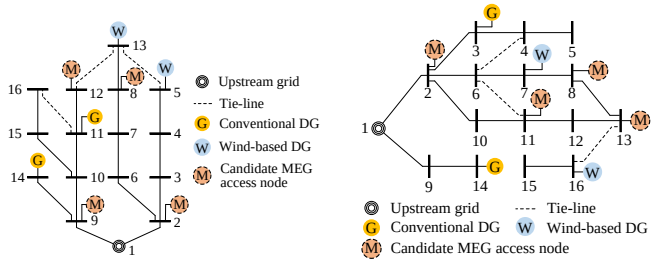

(a) DNS1, DNS3 (b) DNS2

Fig. 6. Wiring schematic diagrams of three DNSs.

and parameters for DNS1 and DNS3 are identical, while their locations in the CTDS are different. The investment cost for hardening distribution line and deploying MEG can be referred in [20] and the deployment cost for automatic switch is set as 5000 $/line. The cost for load shedding and wind power curtailment are set as 2 $/kW and 0.1 $/kW in DNS. The investment budgets for line hardening are set as 180 k$.

To apply the BPHA approach, 4 scenario bundles are selected to implement resilient planning in turn within each iteration of BPHA. And each scenario bundle contains 3 scenarios which is composed of 2 typhoon scenarios and 1 normal scenario. The probability of each bundle can be obtained by adding the probability of typhoon scenarios and normal scenario in the bundle. For ADMM parameters, convergency thresholds ε_1 and ε_2 are set as 0.01. For BPHA parameters, convergency threshold $\varepsilon^{\mathrm{BPHA}}$ is set as 0. Risk preference factors for TNS and DNSs are all set as 0.6 and the confidence level is 0.9. The MIP gap for Gurobi is 0.1%.

(1) Comparative analysis of planning results

To validate the effectiveness of the proposed decentralized resilience enhancement planning method, isolated planning is also conducted to obtain the results. For isolated planning, resilient planning is initially implemented for all the DNSs. Then the transmitted power for each DNS is considered as a constant load in TNS to perform resilient planning of TNS. Both approaches are implemented by solving the planning model using the BPHA method integrated with ADMM.

The planning schemes are shown in Table II. Both approaches yield similar planning schemes for TNS except one more hardened line in isolated planning, which necessitate the hardening of three existing lines and the construction of two candidate lines. The additional hardened transmission line 1-4 is needed in isolated planning due to the disregard of boundary information exchange between TNS and DNS1. Hence, the potential for harnessing self-supply capability in DNS1 and DNS3 with DGs and available MEGs remains unexplored in isolated planning. The schemes in DNSs obtained through two approaches exhibit differences in line hardening, wherein a reduced overall number of hardened lines is obtained for DNS3 in isolated planning. Besides, decentralized planning approach involves the deployment of two MEGs in DNS1, whereas no MEG is deployed in DNS1 in isolated planning. This is because in isolated planning, DNS primarily facilitates power distribution by leveraging power from the upstream TNS without considering the benefits of the it. In contrast, decentralized planning consolidates the overall resilience of CTDS, where the DNS planners deploy MEGs to

This article has been accepted for publication in IEEE Transactions on Industry Applications. This is the author's version which has not been fully edited and content may change prior to final publication. Citation information: DOI 10.1109/TIA.2025.3546909

TABLE II
COMPARISON OF PLANNING SCHEMES FOR TWO APPROACHES

System	Measures	Isolated	Decentralized
TNS	Hardening	1-4, 2-3, 2-6, 4-6	2-3, 2-6, 4-6
	Expansion	1-4, 2-6	1-4, 2-6
DNS1	Hardening	2-6, 9-14, 12-13	2-6, 9-14, 12-13
	MEG	/	Two MEGs
	Automatic switch	/	15-16
DNS2	Hardening	2-10, 4-6, 6-7, 7-8, 8-13, 9-14, 12-13, 13-16, 15-16	2-6, 4-6 6-7, 7-8, 8-13, 9-14, 12-13, 13-16, 15-16
	MEG	Two MEGs	Two MEGs
	Automatic switch	8-13	8-13
DNS3	Hardening	2-6, 6-7, 7-8, 8-13, 9-14, 10-15 11-16, 12-13, 15-16	2-6, 5-13, 6-7, 7-8, 8-13, 9-10, 9-14, 11-16, 12-13, 15-16
	MEG	Two MEGs	Two MEGs
	Automatic switch	15-16	15-16

TABLE III
COMPARISON OF PLANNING RESULTS FOR TWO APPROACHES

System	Results	Isolated	Decentralized
TNS	Investment cost (M$)	3.91	3.28
	Operation cost in NS (M$)	1399.60	1244.24
	CVaR (MW)	2.19	0.08
DNS1	Investment cost (k$)	43.94	57.61
	Operation cost in NS (k$)	23693.18	21283.06
	CVaR (kW)	0	0
DNS2	Investment cost (k$)	192.37	192.37
	Operation cost in NS (k$)	21976.77	21976.77
	CVaR (kW)	0	0
DNS3	Investment cost (k$)	145.49	167.95
	Operation cost in NS (k$)	21289.76	21283.06
	CVaR (kW)	173.15	57.42

(TS: typhoon scenario, NS: normal scenario)

provide emergency power supply under typhoon scenarios and conserve the upstream power supply from TNS to support other buses. Due to various investment options for MEG in DNS1, automatic switch planning schemes also differ in the two approaches.

Table III lists the planning results of two approaches for CTDS. Since one excessive line hardening is avoided under decentralized planning scheme of TNS, the investment cost in TNS is reduced by 0.63 M$ compared to isolated scheme. Due to the supportive role of DGs and deployed MEGs in three DNSs under decentralized planning scheme, sufficient power can be transmitted to other nodes of the transmission network. As a result, expected load reduction and CVaR of TNS under decentralized planning scheme in typhoon scenarios is reduced significantly by about 96% compared to isolated planning scheme. A similar situation is also observed in DNS3. In addition, operation cost of TNS in normal scenarios exhibit a decline in decentralized planning with the boundary information exchanged, which is also observed in DNS1 and DNS3. The investment costs in three DNSs under decentralized planning scheme are lower compared to those under the isolated planning scheme, primarily caused by the disparity of investments in line hardening and MEGs. But such increase can lower the load reduction risk and operation cost. In sum, the resilience in CTDS against typhoons and the economics in satisfying the growing electricity demand are enhanced by decentralized planning.

The boundary transmitted power between TNS and DNSs presents differences when adopting isolated planning and

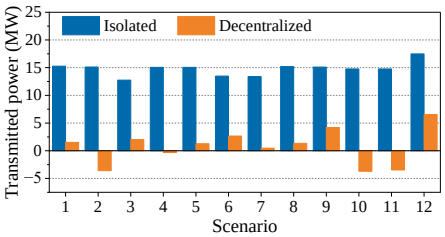

(a) TNS and DNS1

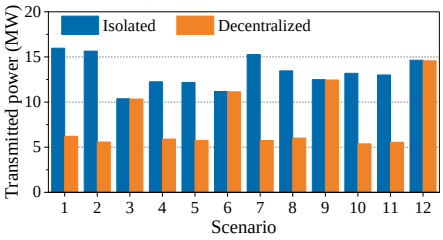

(b) TNS and DNS2

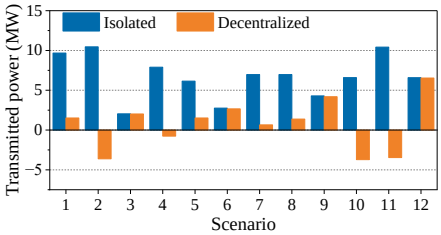

(c) TNS and DNS3

Fig. 7. Power transmitted between TNS and three DNSs of the two approaches.

decentralized planning approaches, which are shown in Fig. 7. The positive transmitted power value indicates that TNS transfers power to DNSs. It can be seen that decentralized planning requires TNS to provide less power supply for DNSs with the support of distributed resources belonging to each DNS. Particularly, the decentralized approach can significantly reduce the transmitted power from TNS to DNS1 and DNS3 in most scenarios, as compared to the isolated approach. This reduction in transmitted power allows for allocation of additional supportive power towards other buses within TNS. Moreover, DNS1 and DNS3 transfer the inverse power flow to transmission network in the scenario 2, 4, 10 and 11 under typhoon impacts. For instance, the power supply of DNS1 and DNS3 in scenario 10 reaches the maximum values of 3.71 MW and 3.72 MW respectively to support TNS in reverse.

The power flow diagram of CTDS after planning in scenario 2 is shown in Fig. 8, which also illustrates the transmitted power between TNS and DNSs. The presented scenario encompasses five typhoon-induced damaged lines in TNS. In response to this catastrophic situation for TNS, three existing lines are hardened and two new lines are constructed. To guarantee the power supply for bus 4 in TNS, electricity generated from the CGU at bus 6 is transmitted to bus 4 with a power injection of 57.43 MW. With the other loads at bus 4 satisfied, a net power injection of 5.27 MW is transmitted to DNS2. And two invested MEGs are deployed at node 2 and 13 respectively with other DGs as well as 8 hardened lines to facilitate power support in DNS2. For the power supply at the bus 1, 3, and 5 in TNS, it is implemented by a power injection

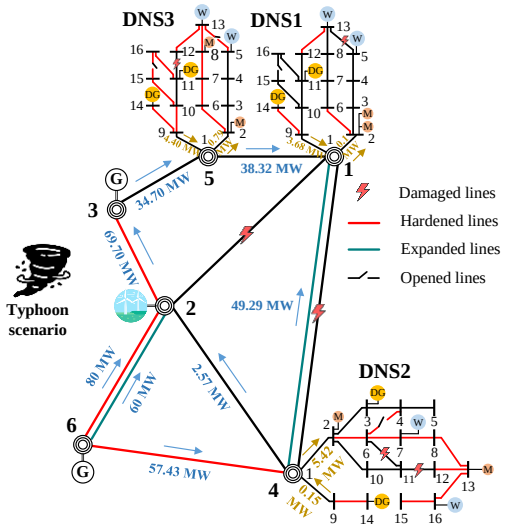

Fig. 8. Power flow of CTDS in scenario 2.

TABLE IV
COMPARISON OF TNS PLANNING RESULTS WITH DIFFERENT RISK FACTORS

TNS risk preference factor	0.3	0.6	0.9
Investment cost (M$)	3.28	3.28	3.97
ELR in TNS (MW)	0.03	0.03	0.01
CVaR (MW)	0.09	0.08	0.04

(ELR: expected load reduction)

of 49.29 MW through the expanded line 1-4 and 69.70 MW through the hardened line 2-3. And by the internal generation resources in DNS1 with two deployed MEGs, the surplus power of 3.58 MW can be generated from DNS1 for other loads at bus 1. Analogously, net power output with 3.61 MW can be generated from DNS3 to transmit the power to DNS1.

(2) Sensitivity analysis of planning results

Table IV compares the planning results of TNS in collaboration with three DNSs under different TNS risk preference factors. It can be seen that the selection of risk preference factors has a direct impact on the results of decentralized planning. As the risk preference factor increases, the planning objective places greater emphasis on mitigating load loss in typhoon scenarios, which leads to the decrease of ELR and CVaR. By allocating additional resources to TNS, the ELR decreases to 0.01 MW and CVaR decreases to 0.04 MW as the risk preference factor increases to 0.9.

In order to investigate the impact of risk preference factor on load reduction risk mitigation performance under typhoon scenarios, load shedding cost is reduced to 50 $/MW for TNS and three DNSs. The specific changes in TNS CVaR with respect to risk preference factors for TNS and DNS are illustrated in Fig. 9. As shown in Fig. 9, the CVaR of TNS maintains a consistent downward trend as the TNS risk preference factor grows, across all settings of DNS risk preference factors. However, for a fixed TNS risk preference factor, an increase in the DNS risk preference factor tends to amplify the TNS CVaR. This is attributed to the fact that a stronger inclination towards mitigating DNS risk might compromise the effectiveness of TNS risk mitigation. For example, TNS CVaR can increase from 0.33 MW to 1.08 MW as all the DNS preference factors grow from 0.3 to 0.9, while keeping the TNS risk preference factor fixed at 0.6. Hence,

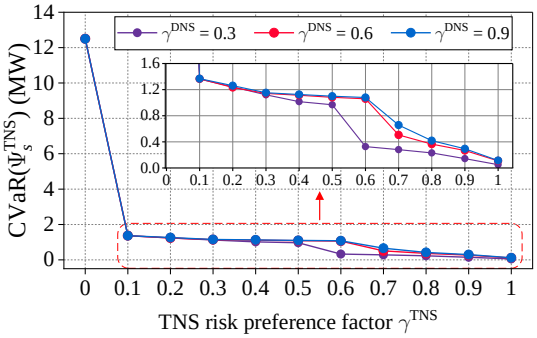

Fig. 9. CVaR of TNS with different risk preference factors.

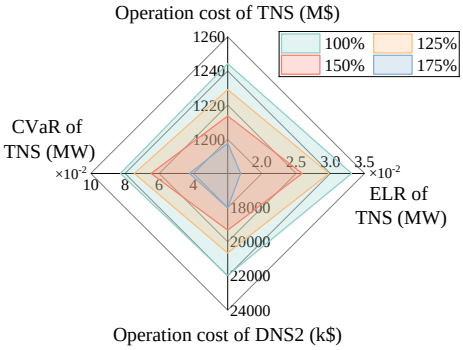

Fig. 10. Operation cost, ELR and CVaR of TNS and DNS2 versus the RDG penetration level in DNS2.

planners can proactively manage the tail risk associated with typhoons by adjusting the risk preference factors of CTDS.

The planning results can also be influenced by the location, renewable-based DG (RDG) penetration of DNS and the network reconfiguration characteristic of DNS. Regarding the DNS location, the divergence in planning results between DNS1 and DNS3 can be attributed solely to variations in typhoon impact, as both possess identical topologies and parameters. The different impact of typhoons results in distinct distribution line failures for DNS1 and DNS3, which leads to the variation of hardening schemes, as presented in Table II, and the variation of CVaR values, as shown in Table III. It reveals the fact that the extent of damage in DNS3 is worse than that in DNS1, thus additional lines need to be hardened and a greater value of CVaR is acquired. It should be noted that despite the differences in hardening schemes and CVaR between DNS1 and DNS3, their boundary exchange power with TNS remains similar due to the identical topologies and parameters, as depicted in Fig. 8.

In order to analyze the effect of RDG penetration level on planning results, four levels of RDG penetration in DNS2 as 100% (normal level), 125%, 150% and 175% are set for comparative analysis. The operation cost, expected load reduction and CVaR of TNS and DNS2 are illustrated in Fig. 10. The tendency shows that an increase of RDG penetration level in DNS2 can directly decrease the operation cost in normal scenarios. Additionally, with the augment of resilience resources in DNS2, the operation cost, ELR and CVaR of TNS is also decreased through the assistance of DNS2.

The planning results, with and without considering network reconfiguration, are compared in Table V. It can be seen that the absence of network reconfiguration necessitates a greater

TABLE VI
COMPARISON OF THE COMPUTATIONAL PERFORMANCE COORESPONDING WITH DIFFERENT SOLUTION METHODS

Solution Methodology	Objective (M$)				Relative error				PHA iterations	CPU time (h)
	TNS	DNS1	DNS2	DNS3	TNS	DNS1	DNS2	DNS3		
ADMM	1303.86	21.34	22.10	21.40	/	/	/	/	/	1.29
BPHA integrated with ADMM	1334.71	21.34	22.17	21.45	2.37%	0.00%	0.32%	0.23%	8	0.27
PHA integrated with ADMM	N/A	N/A	N/A	N/A	N/A	N/A	N/A	N/A	100	5.03

TABLE V
COMPARISON OF PLANNING RESULTS WITH AND WITHOUT CONSIDERING NETWORK RECONFIGURATION

Results	Consider	Not consider
Investment cost of DNS1 (k$)	57.61	80.07
Operation cost of DNS1 (k$)	21283.06	21543.16
CVaR of DNS1 (kW)	0	0
Investment cost of TNS (M$)	3.28	3.28
Operation cost of TNS (M$)	1244.24	1248.45
CVaR of TNS (MW)	0.08	0.1

number of distribution lines in DNS1 to be hardened in order to maintain the radial topology of the distribution network, thereby escalating investment cost from 57.61 k$ to 80.07 k$. Furthermore, the lack of network flexibility results in increased operation cost for DNS1. For TNS, network reconfiguration facilitates the flexible interaction between TNS and DNS1, thereby enhancing the load supply capability and reducing the operation cost. The lack of network reconfiguration increases the CVaR of TNS from 0.08 MW to 0.1 MW.

(3) Validation in efficiency of the solution methodology

To validate the effectiveness of the proposed BPHA method integrated with ADMM. We implement two other solving methods to solve the model based on risk-based decentralized programming model, which are the directly-adopted ADMM and the common PHA integrated with ADMM. The computation performances of different solving methods are compared in Table VI. It should be noted that ADMM yields the original planning results which requires no scenario-decomposition of the formulated model. Hence, the objectives acquired by the ADMM are the baseline solutions, and other PHA methods are compared with them. From Table VI, it can be seen that the proposed BPHA method integrated with ADMM converges with 8 PHA iterations. The computation time for implementing BPHA integrated with ADMM needs 0.27 hours, which is decreased by about 79.1% compared to the ADMM with 1.29 hours. The objective achieved by the proposed method present a relative error of 2.37% for the planning problem of TNS, while very slight errors are present for the planning problems of DNS1, DNS2, and DNS3. For the PHA method integrated with ADMM, it fails to converge for PHA with the non-diminishing termination criterion after 84th iteration, which still remains above the convergency threshold. The total 100 iterations incur a computation time of 5.03 hours. This can be attributed to the significant disparity in risk-based decentralized optimization outcomes between typhoon scenarios and normal scenarios. And the result demonstrates the suitability and superiority of the proposed BPHA method in addressing such resilience enhancement planning problem. The iteration process of the proposed BPHA integrated with ADMM is illustrated in Fig. 11, where the convergency tendency of BPHA is demonstrated through

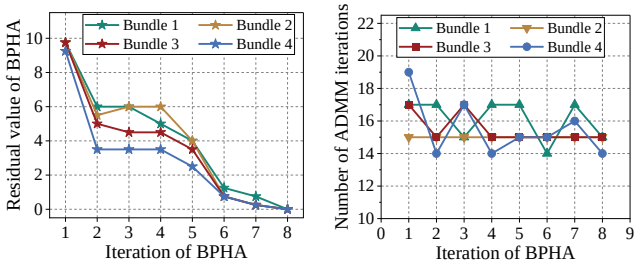

(a) Residual value (b) Number of ADMM iterations

Fig. 11. Iterative process of the solution methodology.

the residual values, and the number of ADMM iterations required during each BPHA iteration is also presented. The residual values of BPHA in each bundle converge to 0 by the 8th iteration, indicating that the planning decisions obtained for the extended RTNSP and RDNSP problems within each bundle eventually become identical. The convergency of ADMM in each iteration of BPHA requires approximately 14-19 iterations for each scenario bundle.

B. T118D7 Test System

The T118D7 test system consists of an IEEE 118-bus transmission network and seven integrated identical distribution networks, including five IEEE 33-bus distribution networks referred to as DNS1, DNS2, DNS3, DNS4, and DNS5, as well as two IEEE 69-bus distribution networks known as DNS6 and DNS7. These aforementioned distribution networks are respectively located at the boundary buses numbered 2, 23, 35, 41, 44, 106 and 117 within the transmission network. The T118D7 test system comprises a total of 421 buses, 693 lines eligible for hardening, 372 candidate lines for construction, 54 conventional generating units (CGUs), 5 wind farms, 30 distributed generations (DGs), 16 candidate MEGs, and other components. The wiring and location schematic diagram of T118D7 system is presented in Fig. A1 with the topologies of TNS, DNS1 and DNS2 displayed, while other DNSs are labeled with their corresponding numbers. Basic transmission network data of IEEE 118-bus system is from [50]. Fifteen typhoon scenarios are generated by Monte Carlo simulation and five normal scenarios are selected to form a total of 20 scenarios. Then four scenario bundles are partitioned, each comprising three typhoon scenarios and one normal scenario, with the respective probability being equal to the sum of individual scenario probabilities. The ratio between normal scenarios and typhoon scenarios is maintained at 9:1. Convergency thresholds for ADMM are set as 0.05. Convergency threshold for BPHA is set as 0. The MIP gap for Gurobi is set as 0.5%.

The planning results are obtained by conducting risk-based decentralized planning and they are compared to the outcomes of isolated planning, as shown in TABLE VII. It can be observed that by implementing the coordination between TNS

TABLE VII
PLANNING RESULTS OF T118D7 SYSTEM

System	Results	Isolated	Decentralized
TNS	Investment cost (M$)	11.38	11.38
	Operation cost in NS (M$)	4298.73	4258.16
	CVaR (MW)	7.67	5.92
DNS1	Investment cost (k$)	74.50	78.57
	Operation cost in NS (M$)	6.87	7.40
	CVaR (kW)	0	0
DNS2	Investment cost (k$)	95.58	99.22
	Operation cost in NS (M$)	3.83	2.93
	CVaR (kW)	0	0
DNS3	Investment cost (k$)	75.38	63.67
	Operation cost in NS (M$)	34.72	36.35
	CVaR (kW)	6.67	11.55
DNS4	Investment cost (k$)	204.69	215.27
	Operation cost in NS (M$)	16.31	17.05
	CVaR (kW)	3.94	0.16
DNS5	Investment cost (k$)	50.42	38.71
	Operation cost in NS (M$)	90.73	82.84
	CVaR (kW)	14.36	30.89
DNS6	Investment cost (k$)	65.33	65.33
	Operation cost in NS (M$)	11.92	13.57
	CVaR (kW)	0	2.81
DNS7	Investment cost (k$)	40.91	33.97
	Operation cost in NS (M$)	11.92	13.68
	CVaR (kW)	0	2.67

and five DNSs in decentralized planning, 22.8% decline in load reduction risks in TNS can be reduced compared to the isolated planning. And a cost of 40.57 M$ can be saved in operation under decentralized planning strategies, despite both approaches having identical investment costs. The above-mentioned benefits of TNS are acquired based on some benefits abandonment in certain DNSs, such as an increase in operation cost by 1.63 M$ and an elevation of load reduction risk in DNS3 from 6.67 kW to 11.55 kW. Nevertheless, decentralized planning enables greater mitigation of overall load reduction risks in CTDS and leads to a decrease in the total operation cost. It is noteworthy that the resilience enhancement benefits of the T118D7 system are achieved through effective coordination between the primary TNS and a limited number of seven DNSs. Further benefits can be exploited in decentralized planning of CTDS by incorporating additional DNSs into collaboration with TNS.

For the computation efficiency, the proposed BPHA integrated with ADMM achieves a computation time of 16.5 hours for solving the risk-based decentralized planning model of T118D7 system, while the directly-adopted ADMM approach fails to converge within 100 hours under the preset MIP gap. To further validate the enhancement of computational efficiency, computational tests are performed with different MIP gaps and ADMM convergency thresholds, where the results are shown in Table VIII and Table IX. For BPHA integrated with ADMM, it is evident that the computation time decreases as the MIP gap and ADMM thresholds increase. However, the ADMM is unable to converge within 100 hours under these conditions except the MIP grows to 3%. Under this condition, ADMM is able to converge requiring a computation time of 75.6 hours, which is significantly longer than that required by the BPHA integrated with ADMM. The result validates the effective performance of

TABLE VIII
COMPUTATIONAL PERFORMANCE WITH DIFFERENT MIP GAPS

MIP gap	BPHA integrated with ADMM		ADMM	
	BPHA iterations	Computation time (h)	ADMM iterations	Computation time (h)
0.5%	21	16.5	N/A	N/A
1%	21	14.1	N/A	N/A
3%	20	9.7	24	75.6

TABLE IX
COMPUTATIONAL PERFORMANCE WITH DIFFERENT ADMM THRESHOLDS

ADMM thresholds	BPHA integrated with ADMM		ADMM	
	BPHA iterations	Computation time (h)	ADMM iterations	Computation time (h)
0.05	21	16.5	N/A	N/A
0.2	21	15.3	N/A	N/A
0.5	21	13.8	N/A	N/A

our proposed solution method when it is applied to a larger and more complicated T&D network system. Despite there still need at least 9.7 hours for the proposed method to address such computational burden, the optimal investment planning scheme for one TNS and seven DNSs, as well as the optimal allocation strategy of resources such as the access node and power output for MEGs in each scenario can be obtained. Besides, more computation time will be reduced using the BPHA integrated with ADMM if the MIP gap increases or the ADMM threshold increases within an acceptable range.

VI. CONCLUSION

This paper proposes a risk-based decentralized planning method of CTDS considering the collaborative effect of TNS and DNSs in defense of stochastic typhoon disasters. The comprehensive planning assets are invested in both transmission and distribution level, encompassing measures of transmission line hardening, transmission network expansion in TNS and distribution line hardening, MEG deployment as well as automatic switch deployment in DNS. For the uncertainties, the randomness of typhoon tracks and electricity growth under normal condition are modeled via multiple scenarios. And the tail risk associated with load reduction resulting from uncertain typhoons is captured using the CVaR metric, enabling a trade-off between resilience performance and investment economics. To address the risk-based decentralized planning model incorporating multiple typhoon and normal scenarios, a novel BPHA approach integrated with ADMM is proposed which can effectively tackle the intricate characteristics of our model and enhance the computational efficiency. By conducting the case studies on a T6D3 system and a T118D7 system, main conclusions can be drawn as:

1) Compared to isolated planning, the proposed decentralized planning approach for CTDS which involves investing assets in T&D network systems, can further mitigate the load reduction risk through the coordination between TNS and DNSs, thereby enhancing resilience against stochastic typhoons. Additionally, this approach also reduces the operation cost of CTDS.

2) Risk preferences for TNS and DNSs can be adjusted for the planner to determine the risk mitigation attitude towards typhoons impact, thereby developing strategic planning

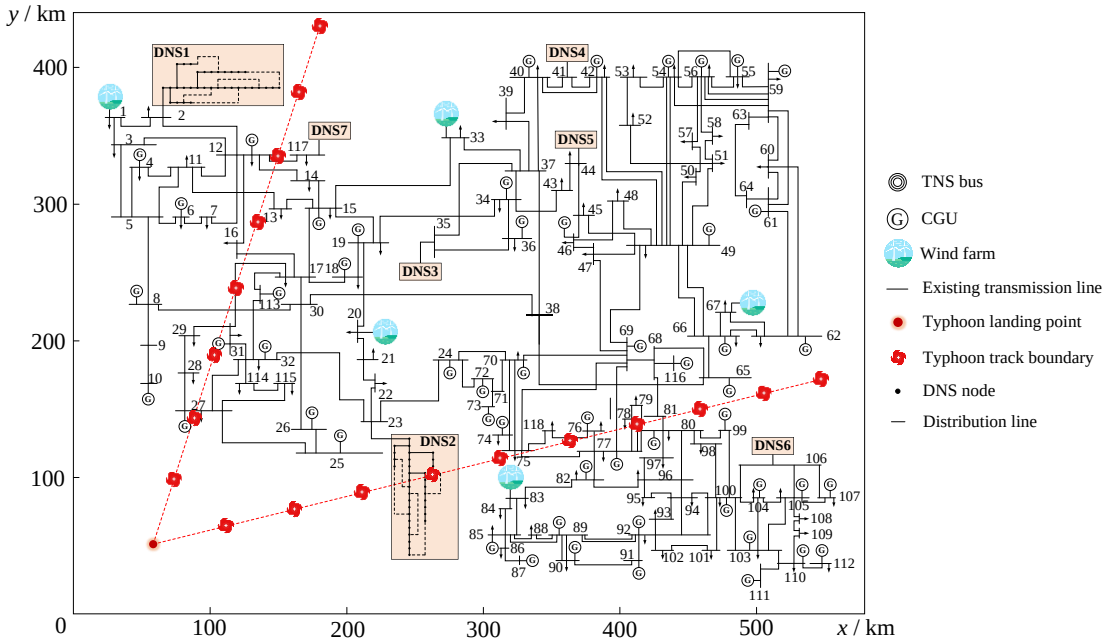

Fig. A1. Wiring and location schematic diagram of T118D7 test system.

schemes for TNS and DNSs according to their expectations.

3) The solution of the risk-based decentralized planning problem with multiple scenarios can be achieved successfully by the proposed BPHA method integrated with ADMM, which is validated on the two test T&D network systems with different scales. And the solution efficiency is greatly improved by the BPHA iteration.

For future work, the involving of time-sequential operation under typhoon scenarios should be explored and incorporated into the present planning model, which can increase its scalability and adjustability. On this basis, spatial-temporal operation strategies such as unit commitment, mobile energy storage system optimization or component maintenance resources dispatch can be considered and incorporated into the planning model, which are also of great importance to system-wide resilience enhancement. Furthermore, the development of more efficient algorithms will remain a key focus in our work to address the resilient planning model of CTDS.

APPENDIX

UPDATE IN THE PENALTY PARAMETERS OF ADMM

To accelerate the iterative process of ADMM, an adaptive penalty method is applied to tune the penalty parameters during ADMM iteration [51], which is shown below.

$$\rho_{o,s,m}^{\mathrm{TNS},(n+1)}=\begin{cases}(1+\varsigma)\rho_{o,s,m}^{\mathrm{TNS},(n)} & \|R_1\|_2\geq\psi\|R_2\|_2\\ \dfrac{\rho_{o,s,m}^{\mathrm{TNS},(n)}}{(1+\varsigma)} & \|R_2\|_2\geq\psi\|R_1\|_2\\ \rho_{o,s,m}^{\mathrm{TNS},(n)} & \text{else}\end{cases} \tag{A1}$$

$$\rho_{o,s,m}^{\mathrm{DNS},(n+1)}=\begin{cases}(1+\varsigma)\rho_{o,s,m}^{\mathrm{DNS},(n)} & \|R_1\|_2\geq\psi\|R_2\|_2\\ \dfrac{\rho_{o,s,m}^{\mathrm{DNS},(n)}}{(1+\varsigma)} & \|R_2\|_2\geq\psi\|R_1\|_2\\ \rho_{o,s,m}^{\mathrm{DNS},(n)} & \text{else}\end{cases} \tag{A2}$$

where ς and ψ are the parameters whose values are set as 1 and 0.1 respectively.

REFERENCES

[1] Li, M. Yang, Y. Tang, Y. Yu and M. Li, "Robust decentralized coordination of transmission and active distribution networks," *IEEE Trans. Ind. Appl.*, vol. 57, no. 3, pp. 1987–1994, May./Jun. 2021.

[2] J. Jasiūnas, P. D. Lund and J. Mikkola, "Energy system resilience - A review," *Renewable Sustain. Energy Rev.*, vol. 150, 2021, Art. no. 111476.

[3] Z. Yuan, H. Zhang, L. Liu, H. Cheng, J. Liu, Y. Wang and D. Cai, "Resilient transmission network hardening planning coordinated with distribution network defensive strategies against typhoons," in *Proc. IEEE/IAS Ind. Commercial Power Syst. Asia*, Chongqing, China, Jul. 2023, pp. 1925-1930.

[4] M. Mahzarnia, M. P. Moghaddam, P. T. Baboli and P. Siano, "A review of the measures to enhance power system resilience," *IEEE Syst. J.*, vol. 14, no. 3, pp. 4059-4070, Sep. 2020.

[5] Y. Li, S. Lei, W. Sun, C. Hu and Y. Hou, "A distributionally robust resilience enhancement strategy for distribution networks considering decision-dependent contingencies," *IEEE Trans. Smart Grid*, vol. 15, no. 2, pp. 1450-1465, Mar. 2024.

[6] Y. Yuan, H. Zhang, H. Cheng and Z. Wang, "Resilience-oriented transmission expansion planning with optimal transmission switching under typhoon weather," *CSEE J. Power Energy Syst.*, vol. 10, no. 1, pp. 129-138, Jan. 2024.

[7] B. Taheri, A. Safdarian, M. Moeini-Aghtaie and M. Lehtonen, "Distribution system resilience enhancement via mobile emergency generators," *IEEE Trans. Power Del.*, vol. 36, no. 4, pp. 2308-2319, Aug. 2021.

[8] F. Rajaei, M. A. Latify and A. Ebrahimi, "Incorporating DSO's situational awareness in resilience-oriented distribution system planning," *IEEE Trans. Smart Grid*, vol. 14, no. 3, pp. 1985-1997, May. 2023.

[9] W. Zhang, C. Shao, B. Hu, K. Xie, P. Siano, M. Li and S. Cao, "Transmission defense hardening against typhoon disasters under decision-dependent uncertainty," *IEEE Trans. Power Syst.*, vol. 38, no. 3, pp. 2653-2665, May. 2023.

[10] A. Bagheri, C. Zhao, F. Qiu and J. Wang, "Resilient transmission hardening planning in a high renewable penetration era," *IEEE Trans. Power Syst.*, vol. 34, no. 2, pp. 873-882, Mar. 2019.

[11] J. Zhou, H. Zhang, H. Cheng, S. Zhang, L. Liu and Z. Wang,

"Resilience-oriented hardening and expansion planning of transmission system under hurricane impact," *CSEE J. Power Energy Syst.*, vol. 10, no. 4, pp. 1746-1760, Jul. 2024.

[12] H. Ranjbar, S. H. Hosseini and H. Zareipour, "Resiliency-oriented planning of transmission system and distributed energy sources," *IEEE Trans. Power Syst*., vol. 36, no. 5, pp. 4114-4125, Jul. 2021.

[13] A. Zare Ghaleh Seyyedi, S. Mahmoudi Rashid, E. Akbari, S. Ashkan Nejati, F. Khalafian and P. Siano, "Co-planning of generation and transmission expansion planning for network resiliency improvement against extreme weather conditions and uncertainty of resiliency sources," *IET. Gener. Transm. Distrib.*, vol. 16, no. 23, pp. 4830-4845, Oct. 2022.

[14] B. Hu, M. Li, T. Niu, P. Zhou, Y. Li, K. Xie and C. Li, "Hardening planning of overhead distribution lines in typhoon-prone areas by considering the typhoon motion paths and the line load reliability," *Int. J. Electr. Power Energy Syst*., vol. 129, 2021, Art. no. 106836.

[15] R. Prakash, B. Lokeshgupta, S. Sivasubramani, T. Kobaku and V. Agarwal, "Optimal DG planning incorporating energy management for an economical and resilient smart distribution system," *IEEE Trans. Ind. Appl*., vol. 60, no. 1, pp. 1890-1901, Jan./Feb. 2024.

[16] C. Wang, K. Pang, M. Shahidehpour, F. Wen and S. Duan, "Two-stage robust design of resilient active distribution networks considering random tie line outages and outage propagation," *IEEE Trans. Smart Grid*, vol. 14, no. 4, pp. 2630-2644, Jul. 2023.

[17] J. Kim, and Y. Dvorkin, "Enhancing distribution system resilience with mobile energy storage and microgrids," *IEEE Trans. Smart Grid*, vol. 10, no. 5, pp. 4996-5006, Sep. 2019.

[18] H. Zhang, S. Ma, T. Ding, Y. Lin and M. Shahidehpour, "Multi-stage multi-zone defender-attacker-defender model for optimal resilience strategy with distribution line hardening and energy storage system deployment," *IEEE Trans. Smart Grid*, vol. 12, no. 2, pp. 1194-1205, Mar. 2021.

[19] S. Ma, L. Su, F. Qiu and G. Guo, "Resilience enhancement of distribution grids against extreme weather events," *IEEE Trans. Power Syst*., vol. 33, no. 5, pp. 4842-4853, Sep. 2018.

[20] S. Ma, S. Li, Z. Wang and F. Qiu, "Resilience-oriented design of distribution systems," *IEEE Trans. Power Syst*., vol. 34, no. 4, pp. 2880-2891, Jul. 2019.

[21] H. Hou, J. Tang, Z. Zhang, Z. Wang, R. Wei, L. Wang, H. He and X. Wu, "Resilience enhancement of distribution network under typhoon disaster based on two-stage stochastic programming," *Appl. Energy*, vol. 338, 2023, Art. no. 120892.

[22] Z. Chen, C. Guo, S. Dong, Y. Ding and H. Mao, "Distributed robust dynamic economic dispatch of integrated transmission and distribution systems," *IEEE Trans. Ind. Appl*., vol. 57, no. 5, pp. 4500-4512, Sep./Oct. 2021.

[23] M. Wang, Y. Wu, M. Yang, M. Wang and L. Jing, "Dynamic economic dispatch considering transmission-distribution coordination and automatic regulation effect," *IEEE Trans. Ind. Appl*., vol. 58, no. 3, pp. 3164-3174, May./Jun. 2022.

[24] G. Muñoz-Delgado, J. Contreras, J. M. Arroyo, A. S. de la Nieta, and M. Gibescu, "Integrated transmission and distribution system expansion planning under uncertainty," *IEEE Trans. Smart Grid*, vol. 12, no. 5, pp. 4113-4125, Sep. 2021.

[25] J. Liu, Z. Tang, P. P. Zeng, Y. Li and Q. Wu, "Distributed adaptive expansion approach for transmission and distribution networks incorporating source-contingency-load uncertainties," *Int. J. Electr. Power Energy Syst*., vol. 136, 2022, Art. no. 107711.

[26] Q. Nguyen, X. Ke, N. Samaan, J. Holzer, M. Elizondo, H. Zhou, Z. Hou, R. Huang, M. Vallem, B. Vyakaranam, M. Ghosal and Y. V. Makarov, "Transmission-distribution long-term volt-var planning considering reactive power support capability of distributed PV," *Int. J. Elect. Power Energy Syst*., vol. 138, 2022, Art. no. 107955.

[27] J. Liu, Z. Tang, P. P. Zeng, Y. Li and Q. Wu, "Fully distributed second-order cone programming model for expansion in transmission and distribution networks," *IEEE Syst. J*., vol. 16, no. 4, pp. 6681-6692, Dec. 2022.

[28] J. Liu, H. Cheng, P. Zeng, L. Yao, C. Shang and Y. Tian, "Decentralized stochastic optimization based planning of integrated transmission and distribution networks with distributed generation penetration," *Appl. Energy*, vol. 220, pp. 800-813, Jun. 2018.

[29] M. Movahednia, R. Mahroo and A. Kargarian, "Transmission-distribution coordination for enhancing grid resiliency against flood hazards," *IEEE Trans. Power Syst*., vol. 39, no. 3, pp. 5272-5282, May. 2024.

[30] Z. Wang, T. Ding, C. Mu, Y. Huang, M. Yang, Y. Yang, Y. Lin and M. Li, "A distributionally robust resilience enhancement model for transmission and distribution coordinated system using mobile energy storage and unmanned aerial vehicle," *Int. J. Elect. Power Energy Syst*., vol. 152, 2023, Art. no. 109256.

[31] Md. S. Miah, R. Shah, N. Amjady, T. Surinkaew and S. Islam, "Resiliency assessment and enhancement of renewable dominated edge of grid under high-impact low-probability events-a review," *IEEE Trans. Ind. Appl*., vol. 60, no. 5, pp. 7578-7598, Sep./Oct. 2024.

[32] H. Jiang, E. Du, N. Zhang, Z. Zhuo, P. Wang, Z. Wang and Z. Yan, "Renewable electric energy system planning considering seasonal electricity imbalance risk," *IEEE Trans. Power Syst*., vol. 38, no. 6, pp. 5432-5444, Nov. 2023.

[33] T. D. de Lima, J. Soares, F. Lezama, J. F. Franco and Z. Vale, "A risk-based planning approach for sustainable distribution systems considering EV charging stations and carbon taxes," *IEEE Trans. Sustain. Energy*, vol. 14, no. 4, pp. 2294-2307, Oct. 2023.

[34] A. Poudyal, S. Poudel and A. Dubey, "Risk-based active distribution system planning for resilience against extreme weather events," *IEEE Trans. Sustain. Energy*, vol. 14, no. 2, pp. 1985-1997, Apr. 2023.

[35] W. Shi, H. Liang and M. Bittner, "Stochastic planning for power distribution system resilience enhancement against earthquakes considering mobile energy resources," *IEEE Trans. Sustain. Energy*, vol. 15, no. 1, pp. 414-428, Jan. 2024.

[36] M. Zare-Bahramabadi, M. Ehsan and H. Farzin, "A risk-based resilient distribution system planning model against extreme weather events," *IET Renew. Power Gener*, vol. 16, no. 10, pp. 2125-2135, Jul. 2022.

[37] A. Poudyal and A. Dubey, "Multi-resource trade-offs in resilience planning decisions for power distribution systems," *IEEE Trans. Ind. Appl*., vol. 60, no. 6, pp. 8031-8043, Nov./Dec. 2024.

[38] H. Zhang, L. Cheng, S. Yao, T. Zhao and P. Wang, "Spatial–temporal reliability and damage assessment of transmission networks under hurricanes," *IEEE Trans. Smart Grid*, vol. 11, no. 2, pp. 1044-1054, Mar. 2020.

[39] X. Liu, K. Hou, H. Jia, J. Zhao, L. Mili, X. Jin and D. Wang, "A planning-oriented resilience assessment framework for transmission systems under typhoon disasters," *IEEE Trans. Smart Grid*, vol. 11, no. 6, pp. 5431-5441, Nov. 2020.

[40] Y. Wang, C. Chen, J. Wang and R. Baldick, "Research on resilience of power systems under natural disasters-A review," *IEEE Trans. Power Syst*., vol. 31, no. 2, pp. 1604-1613, Mar. 2016.

[41] E. Hossain, S. Roy, N. Mohammad, N. Nawar and D. R. Dipta, "Metrics and enhancement strategies for grid resilience and reliability during natural disasters," *Appl. Energy*, vol. 290, 2021, Art. no. 116709.

[42] U.S. Department of Energy, Hardening and Resiliency: U.S. Energy Industry Response to Recent Hurricane Seasons, Tech. Rep., Aug. 2010 [Online]. Available: http://www.oe.netl.doe.gov/docs/HR-Report-final-081710.pdf

[43] Y. Shen, S. Zhang, M. Ding, H. Cheng, C. Li and D. Liu, "Expansion planning of soft open points based distribution system considering EV traffic flow," *IEEE Trans. Ind. Appl*., vol. 60, no. 1, pp. 1229-1239, Jan./Feb. 2024.

[44] R. T. Rockafellar and R. J.-B. Wets, "Scenarios and policy aggregation in optimization under uncertainty," *Math. Operations Res.*, vol. 16, no. 1, pp. 119–147, 1991.

[45] D. Gade, G. Hackebeil, S. M. Ryan, J.-P. Watson, R. J.-B. Wets, and D. L. Woodruff, "Obtaining lower bounds from the progressive hedging algorithm for stochastic mixed-integer programs," *Math. Program.*, vol. 157, no. 1, pp. 47–67, 2016.

[46] R. E. C. Gonçalves, E. G. Finardi, and E. L. D. Silva, "Applying different decomposition schemes using the progressive hedging algorithm to the operation planning problem of a hydrothermal system," *Elect. Power Syst. Res*., vol. 83, no. 1, pp. 19–27, Feb. 2012.

[47] R. Villasana, L. Garver, and S. Salon, "Transmission network planning using linear programming," *IEEE Trans. Power App. Syst.*, vol. PAS–104, no. 2, pp. 349–356, Feb. 1985.

[48] J. Yan, B. Hu, K. Xie, J. Tang and H. Tai, "Data-driven transmission defense planning against extreme weather events," *IEEE Trans. Smart Grid*, vol. 11, no. 3, pp. 2257-2270, Nov. 2020.

[49] H. Zhang, S. Zhang, H. Cheng, Z. Li, Q. Gu and X. Tian, "Boosting the power grid resilience under typhoon disasters by coordinated scheduling of wind energy and conventional generators," *Renew. Energy*, vol. 200, pp. 303-319, Nov. 2022.

[50] "Data for IEEE 118-bus system," IIT, Chicago, IL, USA. [Online]. Available: http://motor.ece.iit.edu/data/Gastransmission_118_14test.xls.
[51] B. D. Biswas, M. S. Hasan and S. Kamalasadan, "Decentralized distributed convex optimal power flow model for power distribution system based on alternating direction method of multipliers," *IEEE Trans. Ind. Appl.*, vol. 59, no. 1, pp. 627-640, Jan./Feb. 2023.

- **Zijun Yuan** received the B.S. degree from Zhengzhou University, China, in 2020 and he is currently working pursuing the Ph.D. degree in electrical engineering with Shanghai Jiao Tong University, Shanghai, China. His research interests include power system planning and power system resilience enhancement.
- **Heng Zhang** received the B.S. degree from China Agricultural University, Beijing, China, in 2014, and the Ph.D. from Shanghai Jiao Tong University, Shanghai, China, in 2019, both in electrical engineering. He is currently an Associate Professor with Shanghai Jiao Tong University. His research interests include power system planning, economic dispatch and power system resilience enhancement.
- **Haozhong Cheng** received the M.S. and Ph.D. degrees in electrical engineering from Shanghai Jiao Tong University, Shanghai, China, in 1986 and 1998, respectively. He is currently a Professor with Shanghai Jiao Tong University. His research interests cover power system and integrated energy system planning.
- **Lu Liu** received the B.S. and M.S. degrees in electrical engineering from Wuhan University, Wuhan, China, in 2006 and 2008, respectively, and received the Ph.D. degree in electrical engineering from Shanghai Jiao Tong University, Shanghai, China, in 2012. Currently, she is an Associate Professor with Shanghai Jiao Tong University. Her research interests include power system planning and assessment
- **Jianqin Liu** received the B.S. degree in electrical engineering from Wuhan University, in 1994. She is currently a Senior Engineering with State Grid Economic and Technological Research Institute., Ltd, Beijing, China. Her research interests include power system planning.
- **Ying Wang** received the M.S. degree in electrical engineering from Zhejiang University, in 2015. She is currently with State Grid Economic and Technological Research Institute., Ltd, Beijing, China. Her research interests include power system optimal allocation.
- **Defu Cai** received the B.Eng. degree and Ph.D. degrees in electrical engineering from the Huazhong University of Science and Technology, Wuhan, China, in 2009 and 2014, respectively. He is currently with Electric Power Research Institute of Hubei Power Grid Corporation, Wuhan, China. His research interests include renewable energy and power system analysis.